Geophys. J. Int. (1999) **136,** 455–476

A spherical harmonic analysis of solar daily variations in the years 1964–1965: response estimates and source fields for global induction—II. Results

Ulrich Schmucker
Geophysikalisches Institut der Universität Göttingen, Postfach 2341, D-37013 *Göttingen, Germany*

Accepted 1998 September 24. Received 1998 September 14; in original form 1998 March 4

SUMMARY

Inductive responses are derived for six harmonics of geomagnetic daily variations, ranging from 24 to 4 hr in period and from 650 to 350 km in penetration depth z^*. Simultaneous data from up to 90 magnetic observatories are involved, and the final results are least-squares estimates with 123 quiet days in a new definition of magnetic quietness. They utilize the potential method of geomagnetic deep sounding, based on series expansions of the magnetic surface field into spherical harmonics, and thus lead to global response estimates in reference to the Earth as a whole.

The analysis is carried out as a univariate linear regression, either between expansion coefficients for the vertical field component and the unseparated potential, or between internal and external potential coefficients, involving assemblages of single days or months. Attempts have been made to remove contamination by lunar daily variations and by internal induction anomalies. The analysis yields response estimates for all spherical harmonic terms in the series, and in the final analysis 12 terms are used for each time harmonic. Estimates for four local-time terms are similar, while those for eight general terms are scattered for the first harmonic, but converge towards higher harmonics. Anomalous effects, as predominantly expected from induction in the oceans, seem to concentrate on low-order time and spherical harmonics, and some degree of lateral uniformity of conductivity apparently exists within the depth range into which daily variations penetrate. This conclusion may be biased towards continents in the northern hemisphere, where most observatories of this study are situated.

The results obtained are nearly the same, whether single days or monthly averages are analysed and whether all days or only quiet days are used. The derived responses for the principal terms of the six time harmonics are compatible with local estimates from other methods, averaged over continental sites, but they are more precise. They agree with responses of a three-layered earth model from a previous joint interpretation of combined *Sq* and *Dst* results. Problems arise with the fifth and sixth time harmonics, which in their spatial structure seem to be detached from the global pattern of daily variations.

Expansion coefficients for the local-time terms on quiet days show a distinct seasonal variability in the form of annual and semi-annual variations, for both their external and their internal parts, which are closely correlated on a day-by-day basis. External coefficients, representative of the four seasons and with corrections for lunar daily variations, are tabulated. Their equivalent currents are displayed on global maps. Special attention is paid herein to the zero reference level in the hypothetical absence of any transient variation field.

Key words: electromagnetic induction, geomagnetic daily variations, Sq source currents.

1 INTRODUCTION

A companion article, henceforth referred to as Part I (Schmucker 1999), presented guidelines for the procedure adopted in this article for the time harmonic and subsequent spherical harmonic analysis of daily variations. The latter provides sets of expansion coefficients to approximate, for a given time harmonic, the potential and the vertical field by two series of spherical harmonics. The analysis is carried out either with the time harmonics of daily variations on a single day or with the time harmonics of mean monthly daily variations.

Section 2 is concerned with the results of the first objective of this study: the derivation of global response estimates with the potential method. Various tests are performed to optimize the choices of days and spherical harmonic terms to be included, and also to check the influence of the changing distribution of observatories having data on a specific day or in a specific month, before final results are presented and compared with results from other methods. Subsequently, in Section 3 attention is directed to the second objective: the time–space structure of daily variations, separated into external and internal parts during quiet times.

This introduction is concluded with a brief review of earth models, which have evolved from global induction research. All of them assume a solely depth-dependent conductivity. It is not clear how representative such models are for the real Earth, with its definite deviations from radial symmetry, at least in the outermost shell of continents and oceans. The potential method, in its first applications by Schuster and Chapman to daily variations (see Part I), revealed unambiguously that the Earth's interior down to some depth is fairly insulating. This could be expected for silicate and oxide-bearing rocks at low to moderate temperatures. They found that below this depth, however, an unexpected rise in conductivity by orders of magnitude *must* occur.

Chapman's (1919) estimates, based on the response for the best-determined second *Sq* harmonic, were 250 km for the thickness of the outer non-conducting layer, and a uniform conductivity of $0.034\ \mathrm{S\,m^{-1}}$ ($28\ \Omega\,\mathrm{m}$) below. Lahiri & Price (1939) found it necessary to add an outermost thin conducting shell to accommodate, besides *Sq*, also *Dst* response estimates. In one of their model options for the deep structure, the non-conducting region extends downwards to 600 km depth, with any conductivity greater than $1\ \mathrm{S\,m^{-1}}$ below. However a more gradual increase of conductivity with depth would also have been compatible with the data.

Modern estimates with different methods, but still utilizing only magnetic data, and with *Dst* responses now over a much enlarged frequency range, confirm the essentials of these early studies, even though there is no longer a stringent requirement for a thin surface shell. Eventually, more structural details may evolve from magnetotelluric response estimates at comparable long periods, even though it appears at present that land-based observations can add only information on phases, and thus lack absolute scaling capability in depth and conductivity.

In the forthcoming analysis, it will occasionally be necessary to refer to a simple representative spherical earth model. The chosen model consists of three layers and is shown in Fig. 1. It comprises an outer shell of 500 km thickness with a conductivity of $0.014\ \mathrm{S\,m^{-1}}$ ($70\ \Omega\,\mathrm{m}$), an intermediate shell of 250 km thickness with $0.063\ \mathrm{S\,m^{-1}}$ ($16\ \Omega\,\mathrm{m}$), and an inner uniform sphere of $2.38\ \mathrm{S\,m^{-1}}$ ($0.42\ \Omega\,\mathrm{m}$). The model gives the best-fitting three-layer interpretation to the responses of the first four *Sq* harmonics in combination with five *Dst* responses for periods from 32 hr to 25 days, all obtained with the $Z:Y$ methods and involving Z at 13 selected continental sites (Schmucker 1985).

2 INDUCTIVE RESPONSE ESTIMATES WITH THE POTENTIAL METHOD

2.1 Basic formulations of the series expansions and of the univariate linear expressions defining responses

The series expansions to be utilized were formulated in Section 4 of Part I: for the magnetic potential U in eq. (6) and for the vertical magnetic field component Z in eq. (7). Their coefficients were defined in eqs (8): $u_n^m(p)$ for U and $z_p^m(p)$ for Z, with n and m denoting degree and order of the respective spherical harmonic, while p indicates the time harmonic, whose Fourier coefficients have been expanded. All spherical harmonic and time harmonic coefficients are to be understood as complex-valued quantities, the latter with local midnight as zero time reference. The usual order of summations is reversed; that is, the first summation in the series is over order and the second over degree, with m fixed.

'Local-time terms' are those of order $m = p$ and degrees $n = p,\ n = p+1, \ldots, p+K-1$, hereafter with the choice $K = 4$, and thus K terms in the second summation. They depend on (geographical) co-latitude θ only, and express the dominant part of daily variations depending on local solar time. The second local-time term with $n = p+1$ is called hereafter the 'principal term', because it is present at all times of the year in more or less the same size and determines the source field structure during equinoxes. All other terms, not following local time, are summarily denoted as 'general terms', with $\exp(\pm i\ell\lambda)$ and $\ell = 1, 2, \ldots, L$ for their dependence on (geographical) longitude λ. Again K terms of ascending degree are used for each order $m = p \pm \ell$, starting with $n = m$. Hence, the choice of a second series parameter $L = 0, 1, \ldots$ defines in $[p-L, p+L]$ the range of orders m for the first summation. Together with the choice of K it yields in $M = K(1+2L)$ the total number of terms.

Response functions with relevance to internal conductivity can be defined in various ways. For the potential method an obvious choice from considerations of causality is a (complex) response function $q_n^m(\omega)$, which expresses *secondary* internal coefficients $\imath_n^m$ in terms of *primary* external coefficients ϵ_n^m, for a given frequency ω and spherical harmonic of degree n and order m. The resulting linear expression is

$$\imath_n^m(\omega) = q_n^m(\omega)\epsilon_n^m(\omega) + \delta\imath_n^m(\omega), \tag{1}$$

where

$$\imath_n^m = \frac{n u_n^m - z_n^m}{2n+1} \quad \text{and} \quad \epsilon_n^m = \frac{(n+1)u_n^m + z_n^m}{2n+1} \tag{2}$$

are the separated internal and external parts of the potential coefficient $u_n^m = \epsilon_n^m + \imath_n^m$, as seen from the Gauss eqs (9) in Part I. By allowing for an internal residual $\delta\imath_n^m$ an univariate linear problem has been formulated, which can be solved by least squares for an assemblage of single-day or mean monthly time harmonics. The resulting estimates of q_n^m are the desired

responses at frequencies $\omega = 2\pi p\ \mathrm{day}^{-1}$ with $p = 1$ to $p = 6$. Appendix A gives details of the least-squares analysis, including errors and weights.

A numerical problem could arise from the fact that the separation formulas eqs (2) involve coefficients from two series expansions of very different quality in the fit to the data, as shown in Section 6 of Part I. The problem can be avoided by relating the expansion coefficients directly, without separation. Using z_n^m as the response to u_n^m, the new linear expression is written as

$$z_n^m(\omega) = [n(n+1)/R]c_n^m(\omega)u_n^m(\omega) + \delta z_n^m(\omega), \tag{3}$$

where R denotes the radius of the Earth. In this alternative formulation, residuals are assigned exclusively to the coefficients of the series expansion for Z, which has the inferior fit to the data. It is readily verified with eqs (2) that the formulas connecting the old and new responses, including errors of their moduli, are

$$\begin{aligned} c_n^m &= \frac{R}{n+1}\,\frac{1-(n+1)/n\cdot q_n^m}{1+q_n^m}, \\ q_n^m &= \frac{n}{n+1}\,\frac{1-(n+1)\cdot c_n^m/R}{1+nc_n^m/R}, \end{aligned} \tag{4}$$

and in a linear approximation

$$\begin{aligned} \Delta c_n^m &= \frac{(2n+1)R}{n(n+1)}\,\frac{\Delta q_n^m}{|1+q_n^m|^2}, \\ \Delta q_n^m &= \frac{(2n+1)n}{n+1}\,\frac{\Delta c_n^m/R}{|1+nc_n^m/R|^2}. \end{aligned} \tag{5}$$

For earth models of radial symmetry, the new response c_n^m, a length, is identical with the C-response, $C_n(\omega)$, in its usual definition for spherical conductors. Hence, $i\omega C_n(\omega)$ is the surface impedance for external source terms of degree n (see Schmucker 1970; Section 5.2), independent of their orders m. This relates the above-introduced responses q_n^m and c_n^m of the potential method to response estimates obtained by other methods, including magnetotellurics, but only in the 1-D case.

As is well known, dependence on degree n is not critical as long as $n|C_n|/R$ is much less than 1; that is, the depth of penetration is small in comparison to the Earth's radius divided by n. Since this will be an important point in the following discourse, Table 1 contains representative model responses for the second time harmonic and varying degrees. Their range corresponds to the henceforth used series expansions with 12 terms ($K = 4$, $L = 1$), which have $n = 6$ as the highest degree for $p = 2$. For completeness, the zero-wavenumber response for a plane earth model is added as an asymptotic value, when $n|C_n(\omega)|/R$ approaches zero with $R \to \infty$ for fixed n. This sequence of model responses indicates that if empirical response estimates c_n^m of varying degrees for the *same* time harmonic are not very different, 3-D effects on the internal part must be small.

Table 1. Inductive response $C_n(\omega)$ of a spherical three-layer earth model (Fig. 1), calculated for the second time harmonic of daily variations and ascending degrees n of the spherical harmonic source term, in kilometres. In the first rows the zero-wavenumber response of an equivalent plane earth model ($R = 6371$ km).

n	C_n	$n\|C_n\|/R$
(0)	536-287i	(0.0)
2	532-274i	0.188
4	522-247i	0.363
6	505-210i	0.514

2.2 Physical implications of response estimates obtained with the potential method, and overview of existing results

Response estimates of the potential method, q_n^m or c_n^m, differ in their implications for internal conductivity from those of any other method. First, they refer to the Earth as a whole, at least formally, and are not localized responses for a specific point of observation. Second, numerous estimates are possible for the same frequency. However, it must be cautioned that the univariate formulations in the above definitions of q_n^m and c_n^m are fundamentally deficient for 3-D earth models. Each external term generates then a full spectrum of internal terms to account for different spatial structures of external and internal parts, the latter being partially determined by possible deviations from radial symmetry in the deep conductivity distribution and by the presence of oceans.

Conversely, each internal term has to be related to all external terms, and a multivariate rather than an univariate linear problem has to be solved. The presumed linearity follows from the linearity of Maxwell's equations. Even in the special case that the inducing source is expressed by one single spherical harmonic, the resulting univariate problem is different from those formulated in eqs (1) and (3) because internal coefficients of *all* degrees and orders have to be related to the external coefficient of degree and order of the source. Hence it could appear as if the subsequently derived univariate responses q_n^m or c_n^m are physically meaningful only under the restrictive assumption of a 1-D earth model, when the postulated one-to-one relationship holds between internal and external coefficients of the same degree and order.

Various attempts will be made to overcome this basic shortcoming of the method in the special case of daily variations: first on the basis that their spectrum of spherical harmonics is dominated by a single term for a given time harmonic, and second from the unique opportunity that these variations offer with respect to the elimination of anomalous internal effects. Since these are fixed to the Earth, the westward-travelling source of daily variations tends to collect the *normal* response for a certain average earth model of radial symmetry.

These considerations underline the importance of evaluating *all* terms of the series expansions. It seems, however, that so far, terms other than the principal terms have received little attention, at least in the context of induction. There are two notable exceptions. Chapman, in a joint analysis of summer and winter data, considered also the external-to-internal ratios of local-time terms with $n = p$ and $n = p + 2$, in the form of their means and semi-differences, which he called 'solstitial mean' and 'solstitial inequality', respectively. Their ratios were found to agree with those of the principal terms (see Chapman & Bartels 1940; Table 4 in chapter XX). Second, Campbell & Anderssen (1983) derived c_n^m values from ratios z_n^m/u_n^m according to eq. (3) for a multitude of spherical terms, with orders up to $m = 4$ and degrees up to $n = 12$. They rejected terms with $|u_n^m|$ below a certain threshold or with arguments of the internal-to-external ratio close to zero or even negative. The responses retained were converted into depths and conductivities of uniform substitute conductors, provided that the argument of

z_n^m/u_n^m was negative and above $-\pi/4$. The results for all terms and harmonics were then displayed jointly in conductivity versus depth diagrams. In this way the authors obtained a fairly consistent conductivity structure for the upper mantle, even though some scatter of individual estimates existed. Campbell & Schiffmacher (1988) extended the work by deriving similar depth profiles separately for a number of continents, conducting a special form of spherical harmonic analysis with data from the respective continent only. In the last-mentioned investigations, however, only ratios for individual data sets were derived, rather than least-squares estimates for assemblages.

For an overview of existing results, Table 2 lists internal-to-external ratios for the principal terms of the first four time harmonics. It begins with Chapman's results. As he gave expansion coefficients z_n^m and u_n^m separately for the two years analysed, the latter from Y only, a rudimentary regression analysis has been conducted, with two data points. The resulting q_n^m estimates are listed together with errors of marginal significance. Parkinson (1977) tabulated his coefficients monthly, and the entries in Table 2 are likewise recalculated least-squares results for the 18 months of the IGY and thus have more meaningful confidence limits. Malin (1973) and Winch (1981) only presented coefficients for the full time spans of their analyses, and the respective table entries are ratios ι_n^m/ϵ_n^m. For comparison, the penultimate column contains the final results from this study.

The overall impression gained from Table 2 is not unfavourable for the potential method, allowing for the fact that different data, different observatories and very different ways of analysing the data are involved. Chapman's and Malin's results, for instance, are not far from the best global response estimates available now, except for the fourth harmonic. In Winch's analysis, problems start with the third harmonic. It is not clear why the estimates from Parkinson's analysis diverge so strongly for all harmonics, deviating from other results far beyond error limits and with no improvements with linear regression. Parkinson's original internal-to-external ratios, which he tabulated month by month and season by season in his Tables VII A–V, give no indication that the disagreement could be connected to any particular month or season.

The last column contains the internal-to-external ratios for the three-layer earth model of Fig. 1. It is fully supported by the response estimates of this study. Their real parts reproduce correctly a postulated maximum at the second and third harmonics, while their imaginary parts increase monotonically with frequency, corresponding to an increasing phase lead of internal from external parts from about 10° at periods of 24 hr to about 30° at periods of 6 hr.

2.3 Tests with respect to the choice of days, observatories and spherical harmonic terms

Now the results of this study will be presented in full detail. They are, as a rule, in the form of complex-valued c_n^m responses in the definition of eq. (4), in units of kilometres. Errors at the 68 per cent confidence level follow in parentheses. They refer to errors of the moduli or to phase errors in radians. Further table entries are the squared coherencies and the number of days, N. In the case of a weighted single-day analysis, the number of days effectively used, N^*, is quoted. It represents the sum of weights and is followed by N in parentheses to indicate the degree to which outliers have been excluded (see Appendix A).

The first test concerns the selection of days and whether mean monthly daily variations or daily variations on single days should be analysed. Table 3 contains a pertinent collection

Table 2. Internal to external potential ratios or response estimates $q_n^m(p)$, derived for the principal terms of order $m = p$, degree $n = p + 1$ and the four time harmonics of daily variations, $p = 1$ to $p = 4$. M is the number of (complex) spherical harmonic terms in the series expansions, and N the number of observatories. Errors refer to the 68 per cent confidence level.

Author		Chapman (1919)	Malin (1973)	Parkinson (1977)	Winch (1981)	This study	Model (Fig.1)
Number of days		362	549-914	90	611	123	
Year(s)		1902 1905	1957-58 (1959)	1957-58	1964-65	1964-65	
M		1	14-18	12	14-20	12	
N		21	100	64	130	74-90	
p = 1 (24 hrs)	Re	0.341	0.369	0.463	0.386	0.374	0.376
	Im	0.069	0.002	-0.013	-0.035	0.052	0.079
	error	(0.078)		(0.013)		(0.004)	
p = 2 (12 hrs)	Re	0.424	0.403	0.465	0.419	0.396	0.388
	Im	0.137	0.118	0.100	0.198	0.140	0.137
	error	(0.042)		(0.021)		(0.005)	
p = 3 (8 hrs)	Re	0.386	0.419	0.321	0.538	0.394	0.391
	Im	0.141	0.161	0.327	0.144	0.169	0.180
	error	(0.022)		(0.055)		(0.008)	
p = 4 (6 hrs)	Re	0.431	0.415	--	0.496	0.372	0.389
	Im	0.109	0.210	--	0.275	0.215	0.209
	error	(0.200)				(0.015)	

Table 3. Principal-term responses $c_n^m(p)$ with $m=2$, $n=3$ for the second time harmonic $p=2$ of daily variations during the IQSY, in kilometres. Errors in parentheses and squared coherencies are for a linear regression with N or effectively N^* days. Results are from six different data sets.

Monthly means	all days:	444 - 238 i (11)	$coh^2 = 0.980$	N = 24
	Q-days:	442 - 230 i (14)	0.985	24
	Q*-days:	439 - 232 i (19)	0.977	20
Single days	all days:	467 - 240 i (5)	0.957	N* = 604 (611)
	Q-days:	478 - 229 i (10)	0.965	119 (120)
	Q*-days:	470 - 236 i (10)	0.966	121 (123)

Notes i.e. all days: all days except the five most disturbed D-days of the month; Q-days: the five quietest Q-days of the month; Q*-days: all quiet days with magnetic activity below a certain threshold (see Part I, Section 3).

of principal-term responses for the second time harmonic, involving days of variable magnetic activity. In addition to the conventional distinction between the five D- and Q-days of a given month, a new and more flexible measure for magnetic quietness was formulated in Section 5 of Part I. Days which qualify under this measure as 'quiet' are hereinafter called Q*-day. With 123 Q*-days and 120 Q-days during the IQSY, quiet days by both definitions are of comparable frequency.

Not surprisingly, the analysis of single days leads to more precise results, but within the same set they all agree in real and imaginary parts within the quoted error limits. It should not be overlooked, however, that the single-day analysis leads to systematically larger real parts. Because coherencies are slightly smaller this cannot be a bias effect. A more likely interpretation is that the monthly means average over changing spatial structures, with unpredictable consequences for the response estimates. The smallness of errors should not be overvalued in any case, since they represent the *statistical* errors. Still, coherencies close to unity testify to an excellent term-by-term correlation between the expansion coefficients of the two series. Even though differences in quality hardly exist, all further results refer to a single-day analysis of Q*-days.

It may have been noted that, with N^* close to N, barely any outliers were encountered when single days were used; that is, the residuals relative to the starting estimates, with unit weights for all days, already have a Gaussian distribution. This is a surprising result of general validity and in clear contrast to experiences with other methods, using for instance as data the locally observed Z in the $Z:Y$ method. It appears that expansions into spherical harmonics have not only a spatial smoothing effect, but they also remove spatially uncorrelated portions in all components.

As an example, the distribution of squared absolute residuals will be examined after the first execution, with the analysis carried out with all days except the 120 D-days of the IQSY. Each of the remaining 611 days is assigned to one of eight classes from $I=0$ (best fit) to $I=8$ (worst fit), as described in Appendix A, eq. (A5). The following numbers are the days contained in the specified class I, with the expected values, rounded off to the nearest integer, following in parentheses:

$I=$	0	1	2	3	4	>4
	432 (418)	115 (132)	42 (42)	12 (13)	5(4)	5(2)

Obviously, in this representative example, weights have to be assigned mainly to those five days in the highest classes, and in the final execution the effective number of days is merely reduced from $N=611$ to $N^*=604$.

The second test examines the influence of observatory positions on the derived responses. A partial answer provides a comparison of results separately for 1964 and 1965. There exists an overlap of 73 observatories with data in both years, but two have data for 1964 only and 16 for 1965 only. Response estimates for the principal terms of the four time harmonics are listed in the first columns of Table 4 for each year.

In some cases disagreements now exceed confidence limits and indicate the presence of systematic errors depending on the choice of observing points. They could arise first from a basic deficiency in approximating the global *Sq* field with only 12 spherical harmonics, or second from localized internal anomalies at sites with data for one year only.

The second columns gives the results for a spherical harmonic analysis with variable weights for the observatories as given in Table 1 of Part I. Almost all estimates increase as if a downward bias had been removed. Even though southern sites with highly anomalous vertical fields now receive double weights, there is almost no reduction in coherency. Hereafter all reported results are with observatory weights in the spherical harmonic analysis.

It may now be asked, whether comparable results could have been obtained with fewer days. This is indeed possible and is demonstrated in the third columns, with responses from the seven Q*-days in September 1964 and the nine Q*-days in October 1965, respectively. Evidently a few quiet days are sufficient to allow fairly accurate estimates, in overall agreement with those for an entire year.

The third test is the most crucial one for methods that involve non-orthogonal series expansions: the influence of the truncation level, here the number M of spherical harmonic terms in the series. Table 5 demonstrates how the estimate for the principal-term response is affected, if this number is varied from $M=1$ for a single local-time term analysis to $M=20$, involving series with four local-time and 16 general terms. It seems as if a break occurs beyond 12 terms, with declining coherencies and with a systematic reduction of absolute values. Both can be ascribed to the onset of numerical instability, which seems to add noise not only to the expansion coefficients for the vertical field, lowering coherencies, but also to potential coefficients, leading to a downward bias of moduli. This test verifies the conclusions of Section 7 of Part I. Hereafter all results refer uniformly to expansion with 12 spherical harmonic terms, that is, with expansion parameters $K=4$ and $L=1$, as a compromise between the desirable allowance of some degree of longitude dependence and numerical stability.

Table 4. Principal-term responses $c_n^m(p)$ with $m=p$, $n=p+1$ for time harmonics $p=1$ to $p=4$ of daily variations on Q*-days. Series expansions are with 12 spherical harmonic terms. Separate least-squares estimates are with $N=76$ observatories in 1964 and $N=90$ in 1965. If observatory weights are used, the sum of weights is given in parentheses below. Errors refer to the 68 per cent confidence level. All entries are in kilometres. Column 1: all Q*-days of the respective year, unit weights for all observatories; columns 2: same, with variable observatory weights; columns 3: same as in column 2, but only Q*-days of one month are used.

		1964			1965		
Number of days		50	50	7	73	73	9
N		76	76	76	90	90	90
			(50)	(50)		(60.5)	(60.5)
	Re	628	672	621	646	669	650
p = 1	-Im	115	115	133	152	169	228
(24 hrs)	error	(18)	(18)	(34)	(14)	(14)	(35)
	Re	486	532	508	468	492	508
p = 2	-Im	218	250	233	247	272	251
(12 hrs)	error	(17)	(17)	(28)	(11)	(11)	(25)
	Re	428	457	469	379	405	404
p = 3	-Im	207	249	224	214	244	211
(8 hrs)	error	(19)	(21)	(32)	(13)	(13)	(23)
	Re	358	368	423	344	361	397
p = 4	-Im	219	265	251	214	249	165
(6 hrs)	error	(24)	(27)	(67)	(23)	(25)	(40)

Table 5. Principal-term responses $c_n^m(p)$ with $m=p$, $n=p+1$ for the pth time harmonics of daily variations, $p=1$ to $p=4$, derived from 123 Q*-days during the IQSY, in kilometres. Response estimates are for four different series expansions with $M=1$ to $M=20$ spherical harmonic terms. Errors are added in parentheses, and squared coherencies are below responses.

	M = 1	M = 4	M = 12	M = 20
p = 1	640 - 167 i (10)	758 - 202 i (11)	669 - 146 i (11)	562 - 192 i (19)
	0.975	0.981	0.972	0.904
p = 2	515 - 282 i (7)	542 - 322 i (9)	509 - 264 i (10)	402 - 257 i (15)
	0.983	0.977	0.970	0.910
p = 3	428 - 278 i (7)	428 - 290 i (10)	426 - 245 i (12)	281 - 180 i (24)
	0.980	0.961	0.942	0.660
p = 4	375 - 267 i (13)	365 - 260 i (17)	365 - 256 i (18)	291 - 223 i (36)
	0.926	0.867	0.852	0.508

2.4 Tests with alternative univariate linear expressions to derive response estimates, including the complete spectrum of spherical harmonics

A last point which needs clarification concerns the formulation of the least-squares problem itself. So far, eq. (3) has been used to derive c_n^m estimates by relating *unseparated* expansion coefficients z_n^m and u_n^m. The justification given for this preference will now be tested by evaluating in the same way and with the same data the alternative formulation eq. (1), in which the q_n^m-response connects *separated* expansion coefficients ι_n^m and ϵ_n^m. Table 6 lists for six time harmonics the resulting two sets of principal-term responses. Quite unexpectedly, the coherency between separated internal and external coefficients turns out to be higher than between unseparated expansion coefficients. For the first four harmonics these improvements are small and the response estimates of the two sets are nearly the same. For the fifth and sixth harmonics, however, differences become substantial. It appears as if the new solution removes underestimations of moduli, which occur when eq. (3) is used. Therefore, the final results of this study in Tables 7 and 8 are c_n^m responses, derived from q_n^m estimates according to eq. (4).

Finally, attention is focused on the complete spectrum of spherical harmonics. Figs 3 and 4 give an impression about the day-to-day correlation between internal and external coefficients in the case of the first time harmonic. For the second time harmonic, the response estimates of the 12 spherical harmonic terms can be found in the upper part of

Table 6. Principal-term responses ($m = p$, $n = p + 1$) for the time harmonics $p = 1$ to $p = 6$ of daily variations, derived from 123 Q*-days during the IQSY. Series expansions are with 12 spherical harmonic terms for each time harmonic. Left column: dimensionless q_n^m response estimates from a regression analysis between internal and external potential coefficients according to eq. (1). right column: c_n^m response estimates, in kilometres, from a regression analysis between unseparated series coefficients according to eq. (3). Errors are added in parentheses, followed by coherencies. To facilitate a comparison, the responses from the first analysis are also listed as converted c_n^m responses, without errors.

	q_n^m	coh^2	(c_n^m)	c_n^m	coh^2
p = 1	0.374 + 0.052 i (.004)	0.988	673 - 146 i	669 - 146 i (11)	0.972
2	.396 + .140 i (.005)	0.984	512 - 264 i	509 - 264 i (10)	0.970
3	.394 + .169 i (.008)	0.963	434 - 246 i	426 - 245 i (12)	0.942
4	.372 + .215 i (.015)	0.888	387 - 260 i	365 - 256 i (18)	0.852
5	.336 + .269 i (.039)	0.533	357 - 285 i	232 - 265 i (38)	0.449
6	.326 + .181 i (.037)	0.491	353 - 173 i	256 - 159 i (32)	0.457

Table 7. Response estimates $c_n^m(p)$ for the complete spectrum of 12 spherical harmonic terms, derived for the second time harmonics $p = 2$ of daily variations on 123 Q*-days during the IQSY, in kilometres Top: results from a univariate analysis according to eq. (1); bottom: results from a bi-variate analysis according to eq. (8). Responses q_n^m have been converted into c_n^m responses with eq. (4). Errors are added in parentheses, and squared coherencies are below responses.

	m = 2	m = 3	m = 1
n = m (univariate)	537 - 296 i (41) 0.880	744 - 118 i (59) 0.549	694 - 842 i (85) 0.834
m+1	512 - 264 i (10) 0.984	525 + 26 i (58) 0.465	1233- 889 i (143) 0.349
m+2	534 - 272 i (41) 0.660	739 - 118 i (58) 0.198	727 - 175 i (55) 0.597
m+3	653 - 479 i (61) 0.422	648 + 95 i (50) 0.182	1116 - 303 i (154) 0.040
n = m (bi-variate)	577 - 235 i (52) 0.921	652 - 66 i (95) 0.574	640 - 755 i (173) 0.834
m+1		652 - 194 i (88) 0.679	1221 - 512 i (192) 0.512
m+2	517 - 249 i (50) 0.750	580 - 107 i (115) 0.240	900 - 12 i (134) 0.643
m+ 3	651 - 230 i (116) 0.494	621 - 68 i (113) 0.232	723 - 156 i (151) 0.352

Table 7. The first column contains the results for the local-time terms ($m = p = 2$); the second and third columns, those for general terms, travelling faster ($m = 3$) and slower ($m = 1$) than the Sun. The effective number of days N^* (not listed) in all estimates is very close to $N = 123$, which is the number of Q*-days in 1964–1965.

The overall agreement in real parts is remarkable and totally unexpected in view of the smallness of many terms, as evident from Figs 3 and 4. Also, the imaginary parts of the local-time terms agree among themselves, while those of the general terms show systematic deviations. Still, with similar results for the other time harmonics, it can be concluded that the response is predominantly 1-D and that the univariate term-by-term analysis has a sound physical basis. The cited encouraging

results of Chapman (1919) and Campbell & Anderssen (1983) have thus been confirmed. Attempts to derive responses for the complete spectrum from the tabulated coefficients in Malin's (1973) and Winch's (1981) works were, however, unsuccessful (Schmucker 1984; pp. 18–19). It will be seen in Section 3 that most spherical terms have a distinct seasonal dependence and that the use of mean daily variations for an entire year leads to uncertain results.

2.5 Attempts to improve response estimates for the principal term

In conclusion, three attempts are described to improve results. The first concerns contributions by lunar daily variations. In the analysis of mean monthly daily variations it can be assumed that such contributions disappear in the average over five or more days of randomly varying lunar phases. This will not be so in the analysis of single days, when each day has its own distinct lunar phase v, henceforth to be understood as lunar phase at noon of the respective day.

With the symbols S and L for solar and lunar daily variations, respectively, the expansion coefficients of a given single day and time harmonic are decomposed as follows:

$$u_n^m = u_n^m(S) + u_n^m(L)\,\mathrm{e}^{-2iv}, \qquad z_n^m = z_n^m(S) + z_n^m(L)\,\mathrm{e}^{-2iv}. \tag{6}$$

The lunar phase factor is for 'phase-law tides', with one solar day as the fundamental period. Details of the underlying physical concept can be found in Appendix B. Even though lunar coefficients are one order of magnitude smaller than solar coefficients in amplitude, they contribute a certain amount of noise to both sides of eqs (3). Assuming that the same coefficients $u_n^m(L)$ can be used for all days, the lunear contamination has a deterministic amplitude, but random phase. It should lower coherencies and lead to underestimations of the response moduli.

Counting days from $n_D = 1$ for 1 January 1964 to $n_D = 731$ for 31 December 1965, the lunar phase on the n_Dth day at Greenwich noon is

$$v(n_D) = v_0 + 12^\circ.19075 n_D, \tag{7}$$

with $v_0 = 59^\circ.09$ as the phase of the Moon on 31 December 1963. The accuracy is quite sufficient for the intended use, noting that the lunar phase increases by about 12° from midnight to midnight. Hence, the evaluation of eq. (6) with eq. (7) and a given set of lunar coefficients for zero phase, here from Winch's (1981) analysis, readily reduces empirical coefficients to those which on the respective day represent exclusively *solar* daily variations.

However, a repetition of the analysis with lunar-corrected spherical terms left the resulting coherencies essentially unchanged, and no indications existed for any removed bias in the response estimates. This negative result may reflect to some extent the use of the same lunar coefficients for all seasons. A second deficiency is the substantial difference in the choice of spherical harmonic terms in Winch's analysis and this study. Both have led to the decision to abstain in this context from any further experiments to remove lunar effects.

The second attempted improvement concerns the separation of travelling and standing modes in pairs of westward- and eastward-moving waves, that is with longitude factors $\exp(im\lambda)$ and $\exp(-im\lambda)$, respectively. If with $|u_n^m| > |u_n^{-m}|$ the westward-moving wave has the larger amplitude then, as shown in Appendix C, the travelling mode of the superposition of both terms is

$$(|u_n^m| - |u_n^{-m}|)\frac{u_n^m}{|u_n^m|}\exp\{i(m\lambda + pt)\},$$

moving westward, whereas the standing mode, with the notation of Appendix C, is

$$2|u_n^{-m}|\cos(m\lambda + \delta)\exp\{i(pt + \sigma)\}.$$

It is reasonable to assume that travelling modes, provided they move westwards with the Sun, are not substantially affected by internal induction anomalies due to oceans and possibly other deep-seated sources of anomalous induction, which are both fixed to the Earth.

A repetition of the analysis with solely westward-travelling modes, however, lowered the coherencies of the response estimates severely. Here the major obstacle seems to be the restriction in the permissible number of spherical terms. To obtain pairs of westward *and* eastward waves, the series expansions had to be reformulated, noting that with the chosen series parameter $L = 1$ not a single eastward wave is included. Various attempts to express both the external field and the anomalous internal field with about 12 terms have been unsuccessful. Hence, the intended separation of normal and anomalous internal parts has to await analyses with more spherical terms and thus the establishment of a more suitable distribution of observing points. Under the given circumstances, similar responses for different spherical terms for the same time harmonic have to suffice as evidence that the derived responses are essentially 'normal', and thereby consistent with spherically symmetric earth models.

The third attempt also concerns anomalous internal effects. Under the simplifying assumption that these effects are linearly related primarily to the leading principal source term, eq. (1) will be replaced for the pth time harmonic by the bi-variate expression.

$$\imath_n^m = \bar{q}_n^m \epsilon_n^m + q_{np+1}^{mp}\epsilon_{p+1}^p + \delta\imath_n^m. \tag{8}$$

It yields for all terms, except the principal term, separate least-square estimates of 'normal responses' $\bar{q}_n^m$ and 'anomalous responses' q_{np+1}^{mp} with respect to the principal source term. For this term itself, normal and anomalous responses are inseparable.

In order to give an idea of how this attempted decomposition modifies the results, normal responses from the bi-variate analysis are listed in the lower part of Table 7, after a conversion into c_n^m responses. A comparison with the univariate results in the same Table 7 shows that the bi-variate formulation improves coherencies in all cases and removes all inconsistencies in the form of positive imaginary parts. Errors are larger now, but this was to be expected from the reduced degrees of freedom of the analysis. In spite of this partial success, the overall usefulness of the bi-variate analysis remains in doubt as long as it has not been tested with 3-D spherical earth models.

2.6 Global responses, apparent resistivities and phases in comparison with the results of the $Z:Y$ method

This section closes with a critical examination of the response estimates, which have been finally obtained for the principal terms. They are listed in the second column of Table 8. Statistical errors up to the fourth harmonic are of the order of a few per cent, and the results are in excellent agreement

Table 8. Inductive response estimates of daily variations for periods between 24 hr ($p = 1$) and 4 hr ($p = 6$). Listed are the principal-term responses $c_n^m(p)$ for the potential method, and mean continental $C_0(\omega_p)$ responses for the $Z:Y$ method; $m = p$, $n = p + 1$, $\omega_p = 2\pi p\ \mathrm{day}^{-1}$. N_D is the number of analysed days, M the number of spherical harmonic terms in the series expansions, N_{SHA} the number of observatories for the spherical harmonic analysis, with their effective number in parentheses, and N_Z the number of observatories used for deriving continental means. Errors refer to the 68 per cent confidence level. C-responses are in km, apparent resistivities ρ_a in Ω m, and phases ϕ of the impedance in degrees.

		Potential method		Z:Y method		Model
		Chapman (1919)	This study	This study	Olsen(1998)	
N_D		362	123	123	1650	
M		1	12	12	120	
N_{SHA}		21	74(50)-90(61)	74(50)-90(61)	90	
N_Z		--	--	59	24	
p = 1	Re	763	673	643	608	660
	-Im	205	146	226	247	219
	error	(227)	(11)	(43)	(23)	
24 hrs	coh^2	--	0.988	0.839	0.94	
	ρ_a	57.0 (32.8)	43.3 (1.4)	42.5 (5.4)	39.4 (5.5)	44.2
	φ	75.0 (16.5)	77.8 (0.9)	70.6 (3.6)	67.9 (2.0)	71.6
p = 2	Re	462	512	477	500	528
	-Im	249	264	283	239	262
	error	(76)	(10)	(34)	(25)	
12 hrs	coh^2	--	0.984	0.814	0.92	
	ρ_a	50.3 (14.6)	60.7 (2.1)	56.2 (6.9)	56.1 (5.1)	63.5
	φ	61.7 (8.3)	62.7 (1.0)	59.3 (3.5)	64.5 (2.6)	63.6
p = 3	Re	455	434	382	432	434
	-Im	209	246	244	244	262
	error	(32)	(12)	(34)	(20)	
8 hrs	coh^2	--	0.963	0.692	0.86	
	ρ_a	68.7 (8.8)	68.2 (3.3)	56.3 (8.4)	67.5 (5.4)	70.5
	φ	65.3 (3.7)	60.5 (1.4)	57.4 (4.3)	60.5 (2.3)	58.9
p = 4	Re	349	387	334	389	371
	-Im	124	260	215	240	247
	error	(224)	(18)	(48)	(17)	
6 hrs	coh^2		0.888	0.455	0.71	
	ρ_a	50.1 (60.6)	79.5 (6.1)	57.7 (13.9)	76.4 (5.7)	72.5
	φ	70.4 (34.7)	56.1 (2.2)	57.2 (6.9)	58.3 (2.1)	56.3
p = 5	Re		357	293	348	326
	-Im		285	116	247	230
	error		(42)	(76)	(18)	
4.8 hrs	coh^2		0.533	0.183	0.56	
	ρ_a		95.3 (17.5)	51.8 (23.3)	83.2 (7.0)	72.9
	φ		51.4 (5.3)	60.5 (13.0)	54.6 (2.4)	54.9
p = 6	Re		353	262	325	295
	-Im		173	115	246	213
	error		(39)	(85)	(19)	
4 hrs	coh^2		0.491	0.115	0.47	
	ρ_a		84.7 (16.8)	44.9 (26.7)	91.1 (8.5)	72.7
	φ		63.9 (5.7)	66.3 (17.0)	52.9 (2.7)	54.2

with the model responses in the last column, demonstrating their high quality and overall compatibility with a radially symmetric earth. Notable disagreements exist only for the imaginary part of the first harmonic which is smaller than expected, and the phase of the sixth harmonic. Coherencies are above those of any other method. This implies that systematic errors should be small, if they occur at all.

The sharp drop in coherency for the fifth and sixth time harmonics was to be expected, not only from the smallness of their amplitudes, but also from the fact that in the series

expansions the dominance of the second local-time term is completely lost (see Fig. 5 in Part I). These harmonics appear as disconnected from the westward-moving global source. From their lowered coherencies it follows that the moduli could be slightly underestimated. In the case of the sixth harmonic, with the lowest coherency of all, the phase also seems to be in disarray.

The remaining entries in Table 8 are the following. The first column contains re-calculated *C*-responses from Chapman's analysis (see Table 2). The best-determined response for the third time harmonic is in remarkably good agreement with all others. In the first harmonic the real response appears as too large, and in the fourth harmonic the imaginary response as too small, even though the deviations are within the cited wide (and unrealistic) error limits. It may be of interest to recall that the model calculations of Lahiri & Price (1939) were based on these *Sq* responses.

In the third and fourth columns of Table 8, results are given from a different method: the $Z:Y$ method, as outlined in Appendix D. It is based on the locally observed vertical field and thus yields *local* rather than *global* response estimates. To allow for a comparison with estimates from the potential method, table entries represent mean responses for selected groups of N_Z observatories. For their derivation, the required Fourier products in eqs (A2) and (A3) are summed first over all days with weights, and then over all selected observatories without weights. The quoted errors do not refer to confidence limits of the listed mean responses. They are to be understood as mean standard deviations of individual observatory responses from the tabulated mean response, in the sense that they have been derived with

$$\nu_2 = 2\sum_k N_k^*/N_Z - 2 \qquad (9)$$

as degrees of freedom in the F-distribution (see Appendix A). N_k^* is the effective number of days at the kth observatory, $k = 1, 2, \ldots, N_Z$.

The $Z:Y$ method requires a spherical harmonic analysis of the horizontal field components, and for the comparison the same set of potential coefficients has been used as in the potential method. For Z all 59 observatories are included, which are classified as 'continental' in Table 1 of Part I. In this way, the entries in the second and third columns arise from the same data except that the $Z:Y$ method does not use Z on islands or coastlines. Since the excluded observatories are well known for their anomalous daily variations in Z, as evident from Fig. 2 of Part I, it might be expected that the $Z:Y$ method leads to systematically different and also to more reliable response estimates.

However this is definitely not the case. Not only do both sets of estimates agree mostly within error limits, but the coherencies for the potential methods are clearly above those of the $Z:Y$ method. Furthermore, the linear relation between expansion coefficients, as used in the potential method, seems to be far more consistent on a day-by-day basis. This is indicated by the smaller number of excluded outliers. For the $N = 123$ Q*-days analysed the effective number of exclusions is $N - N^* = 4$, or less for all six harmonics, when the potential method is used. Hence, its residuals already are more or less normally distributed without weights, indicating about the same degree of correlation on all days. In contrast, a substantial day-by-day variability of correlation exists for the $Z:Y$ method. In the case of the first harmonic, with $N^* = 56$, more than one-half of the available data have to be excluded before an acceptable distribution of residuals is obtained. For the higher harmonics the exclusions are less stringent, but still well above the level required in the potential method. Their smallest number is $N - N^* = 21$ exclusions for $p = 6$. The quoted values for N^* refer to an average over all N_Z observatories.

Since the $Z:Y$ method does not involve a spherical harmonic analysis of Z, all calculations have been repeated with $M = 20$ potential terms, which is still within the tested range of numerical stability. However, this improved global approximation to the horizontal components does not change the outcome to any measurable degree. Furthermore, a repetition with the 24 European observatories in Olsen's (1998) analysis has led to essentially the same results.

Olsen's results have been added in the fourth column of Table 8 to allow for a comparison with an independently derived set of responses. They are reproduced from Table 3 of the cited publication, after a few computational corrections. The quoted coherencies are from Olsen's Table 2 for the observatory Fürstenfeldbruck. Since this is a typical continental site, they should be equivalent to the coherencies obtained in this study. Olsen analysed many more days, including those of this study, and found it necessary to lower substantially their effective number by weights. The spherical harmonic analysis of horizontal components was carried out with a comparable set of observatories, but Olsen increased the number of spherical terms by a factor of 10, which forced him to use a generalized inverse of the normal equation matrix, a complication deliberately avoided in this study. Errors refer again to standard deviations with respect to the listed mean responses of 24 European observatories, all of them continental.

In spite of the fact that Olsen's results were obtained in a very different way, up to the fourth harmonic the agreement with this study is good. Only the (negative) imaginary response of the first harmonic is significantly larger, even though it should be noted that it varies greatly among subsets of observatories, from less than 200 km to almost 400 km, as seen in Olsen's Fig. 4. Coherencies are slightly above those obtained with the $Z:Y$ method in this study, but they still do not reach the coherencies that are attainable with the potential method. The thus established agreement of global and averaged local responses is not self-evident and is an indication for a laterally rather uniform upper mantle. However this notion should be treated with the reservation that geomagnetic surface fields represent the tangential electric mode of the induced fields and thus may not be too sensitive to lateral non-uniformities at depth.

Olsen's reponses are not directly comparable as far as absolute values are concerned. He has multiplied his least-squares estimates with certain (real) factors $f(\eta) > 1$ to reduce systematic underestimations from presumed errors in the input variable Y, adopting a certain ratio η of errors in Y and Z. For a given coherency this factor is

$$f(\eta) = \frac{1-\eta}{2} + \sqrt{\left(\frac{1+\eta}{2}\right)^2 + \eta b} \quad \text{with} \quad b = 1/\mathrm{coh}^2 - 1\,, \qquad (10)$$

corresponding to Olsen's eq. (23).

In the case of the first three time harmonics, coherencies are so close to unity that bias corrections hardly matter, when

with $b \to 0$ and with Olsen's well-founded choice of $\eta = 0.25$ the correction factors approach one.

Now an attempt will be made to correct the response estimates of this study for the last three harmonics, which have coherencies well below unity, adopting the cited value for η. Observing that phases remain unchanged, the real parts of the corrected responses, that is to say the depth values z^*, are quoted, in kilometres, for $p = 4$ to $p = 6$. In the case of the potential method they increase from 387, 357, 353 to 450, 412, 416, and in the case of the $Z:Y$ method from 334, 293, 262 to 404, 439, 498. Evidently, the bias correction restores to some extent the agreement among estimates, but it destroys their compatibility with 1-D models in the sense that z^* should decrease with increasing frequency. Hence, no bias-correction will be used.

For completeness, Table 8 also contains for each response the apparent resistivity and phase of the impedance in the definitions

$$\rho_a = \omega\mu_0|C|^2 \quad \text{and} \quad \varphi = \pi/2 + \arg\{C\}, \tag{11}$$

including errors $\Delta\rho_a = 2\rho_a \Delta C/|C|$ and $\Delta\varphi = \Delta C/|C|$; C stands for c_n^m or C_n. Fig. 1 provides a visual display of all results in the form of a $\rho^*(z^*)$ diagram, in which for each harmonic

$$\rho^* = \rho_a 2\cos^2\varphi (\varphi \geq \pi/4) \quad \text{or} \quad \rho^* = \rho_a/[2\sin^2\varphi] (\varphi < \pi/4) \tag{12}$$

associates a resistivity estimate ρ^* with the depth $z^* = \mathscr{R}e\{C\}$ of a perfect substitute conductor. The three-layer model and its responses are also shown.

The data points demonstrate most clearly the well-established transition in mantle resistivity between 400 km and 800 km depth from values near to 100 Ω m to values below 1 Ω m. It may occur in two steps at 500 km and 750 km depth, as in the model, or in one single step around 600 km, or with a smooth descent starting at 400 km and ending below 800 km. For the first harmonic, scattered ρ^* values again indicate problems with phase determinations, and general uncertainties exist with the last two harmonics. For the second to fourth harmonics, empirical and model values in z^* and ρ^* are in almost perfect agreement.

So far, only responses for the principal terms have been examined. Fig. 2 provides an overview of responses for the complete set of evaluated terms: 11 for the first time harmonic and 12 for each of the higher harmonics, yielding a total of 71 response estimates for six frequencies. They are from a bi-variate analysis according to eq. (8) and are shown in the same style of ρ^*–z^* diagrams as in Fig. 1, but to avoid confusion separately for each time harmonic. The principal responses determined by univariate regression and already displayed are added for completeness. Points on the depth axes refer to those two estimates of c_n^m for which ρ^* is below 1 Ω m.

Even though data points are scattered, it is impressive to observe how they gradually converge when p and thereby the frequency increases. It seems as if internal induction anomalies, presumably mostly from oceans, contribute mainly to spherical terms of low orders and degrees, when the penetration depth is large and the anomalous effects spatially widespread. Higher harmonics, in contrast, show much more uniform responses, which are in overall agreement with the respective 1-D model responses. In the apparent absence of ocean effects, this could suggest a high degree of lateral uniformity within the penetrated depth range of the Earth's uppermost continental mantle. However it should be cautioned that low-order and low-degree spherical harmonics were not used in the analysis of higher

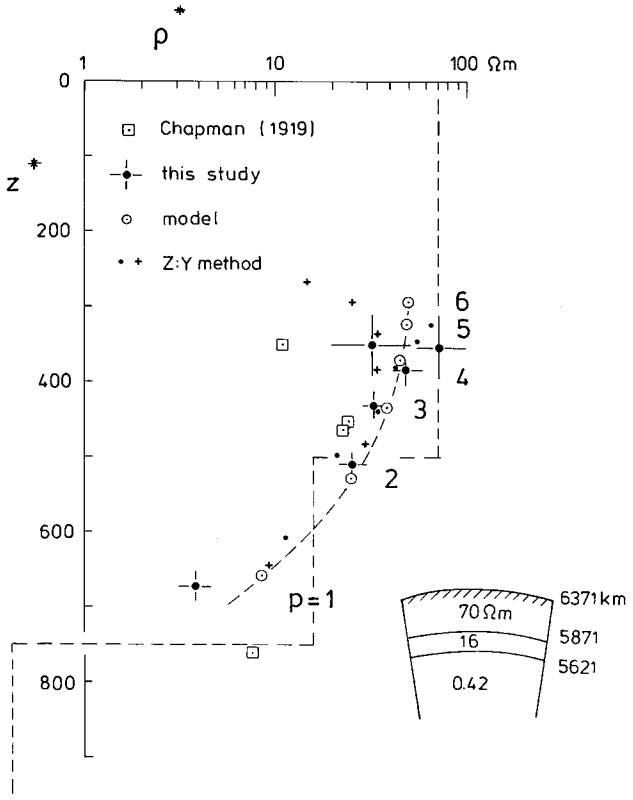

Figure 1. Global response estimates of this study for the six time harmonics of daily variations, from $p = 1$ (24 hr period) to $p = 6$ (4 hr period), obtained with the application of the potential method to the principal spherical harmonic term of each time harmonic. Also displayed are Chapman's (1919) results and responses for a spherical three-layer earth model, shown in the lower right corner. The newly derived responses improve the overall compatibility with 1-D models and extend the estimates to $p = 6$. Best agreements between calculated and empirical responses exist from the second to the fourth harmonic, for the adopted model. Divergent ρ^*-values for the first harmonic. Mean continental responses from the $Z:Y$ method are added for comparison, omitting error bars. Dots represent Olsen's results; crosses, results from this study. All the responses shown are listed in Table 8. The display is in the form of apparent resistivity versus depth profiles, in which for each harmonic a resistivity ρ^* is assigned to the depth z^* of a perfect substitute conductor. (See text for details.)

time harmonics, noting that in the case of the pth harmonic the lowest degree and order are $p - 1$.

From Fig. 2 it is also evident that local-time term responses tend to be clustered around model responses. An exception is the wide range of ρ^*-values for $p = 1$, where again the problem lies with uncertain phase determinations. Hence, the unfavourable impression of strongly divergent results in Fig. 2 arises mainly from the general terms. It is also noteworthy that up to $p = 4$ the principal term has by far the best determined response, but that for $p > 4$ this distinction is lost, with error bars of about the same length for all local-time terms.

3 EXTERNAL AND INTERNAL FIELD PRESENTATIONS

There are two possible ways of finding the external part ϵ_n^m of a given unseparated potential coefficient $u_n^m = \epsilon_n^m + \iota_n^m$: (1) by converting also the vertical component Z into series of spherical harmonics, which allows the use of Gauss's separation formula

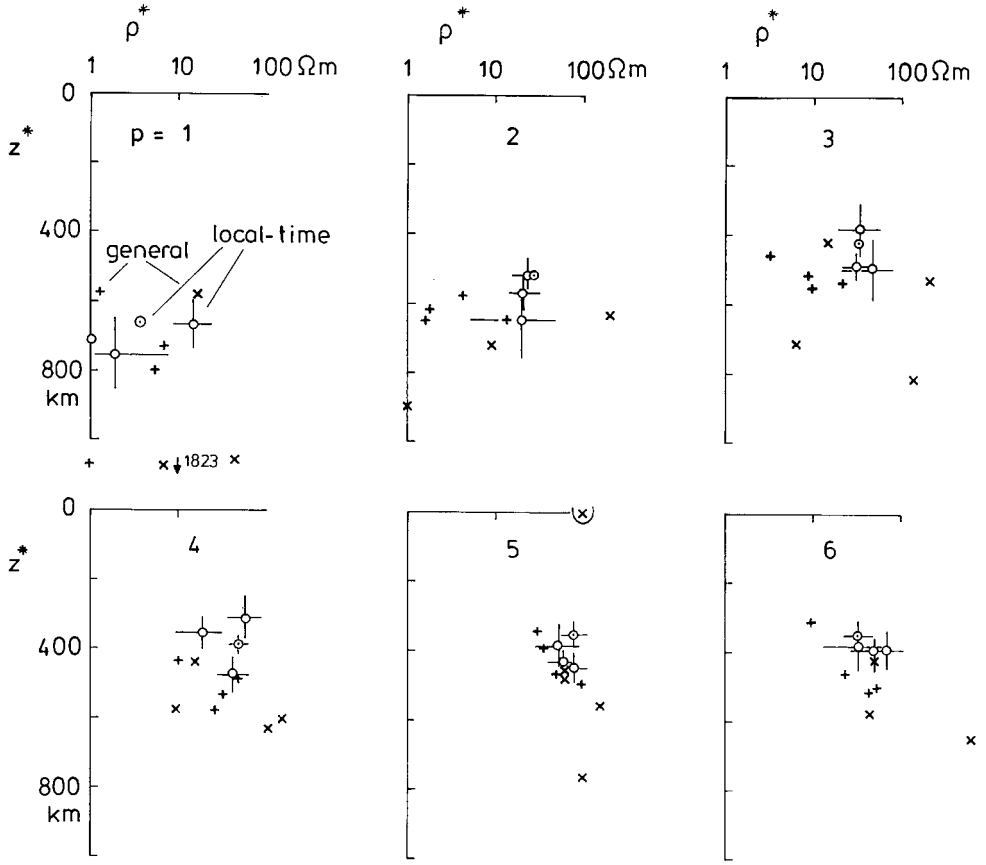

Figure 2. Response estimates for the complete spectra of spherical harmonics, presented in similar $\rho^* - z^*$ diagrams to in Fig. 1. There are 12 spherical harmonic terms for each time harmonic $p = 1$ to $p = 6$: four local-time terms of order $m = p$ with error bars (open circles), eight general terms without error bars (crosses), i.e. four terms with $m = p + 1(+)$ and four terms with $m = p - 1(\times)$. Principal-term responses ($m = p$, $n = p + 1$) are marked by a dot within the circle. Up to $p = 3$ there is good agreement among the four local-time term responses except for some phase problems with the first harmonic. Converging responses for *all* terms beyond $p = 3$ indicate diminishing anomalous effects from oceans and possibly other lateral non-uniformities in the upper mantle.

eq. (2); (2) by assuming an earth model of radial symmetry, which with $Q_n = \iota_n^m/\epsilon_n^m$ as internal to external model ratio yields in $\epsilon_n^m = u_n^m/(1 + Q_n)$ the desired external part. Both options have been tested and only marginal differences were found. Hereafter all cited results have been obtained with the assumption-free first option. Internal coefficients from Gauss's second formula are added for completeness.

For an overview, Fig. 3 presents external and internal potential coefficients for the analysed sequence of 123 Q*-days during the IQSY, displaying the real parts of these coefficients day after day for the four local-time terms of the first time harmonic. Even though some scatter exists, a distinct seasonal modulation is visible. For the equator-symmetric terms with P_1^1 and P_3^1 it occurs in the form of annual variations, and for the equator-antisymmetric terms with P_2^1 and P_4^1, in the form of weak semi-annual variations, which are superimposed on time-constant major portions. Most impressive is the strong seasonal variability of the P_1^1 term, which passes through zero during equinoxes and thus is responsible for most of the hemispherical imbalance during solstices. At these times the P_1^1 term exceeds in size even the principal second term P_2^1.

Within the two years analysed, the coefficients of the seven general terms also undergo some systematic seasonal changes, as seen in Fig. 4. The overall impression is that all coefficients vary smoothly with progressing time, except for their scattered appearance in the case of the P_1^0 term, which has no longitude dependence in Universal time. The reason for the scatter is unclear, but contributions from the *Dst* continuum at the 24 hr period would be a possibility. Noteworthy in Figs 3 and 4 is the well-correlated seasonal variation of external and internal parts, even to small details in day-by-day changes, which corresponds to the high degree of coherency found in the statistical analysis.

One further preliminary note is necessary with regard to the absolute term in the time harmonic analysis, which is here identical to daily means measured from the local midnight level. For a physically meaningful representation of external source fields these absolute terms have to be taken into account and likewise separated into external and internal parts after a spherical harmonic analysis. This point has been thoroughly dealt with in Appendix A to Part I. For the analysis the same expansion series will be used as formulated for the time harmonics, setting $p = 0$ in eqs (6) and (7) of Part I and observing that the absolute terms are real quantities. Hence, expansion coefficients of positive and negative orders must be complex conjugates, and the series can be restricted to positive orders. This leads to the formulation

$$U_0(\theta, \lambda) = R\left\{\sum_{n=1}^{K-1} u_n^0 P_n(\cos\theta) + \sum_{m=1}^{L}\sum_{n=m}^{m+K-1} \mathcal{R}e[u_n^m \, e^{im\lambda}] P_n^m(\cos\theta)\right\} \quad (13)$$

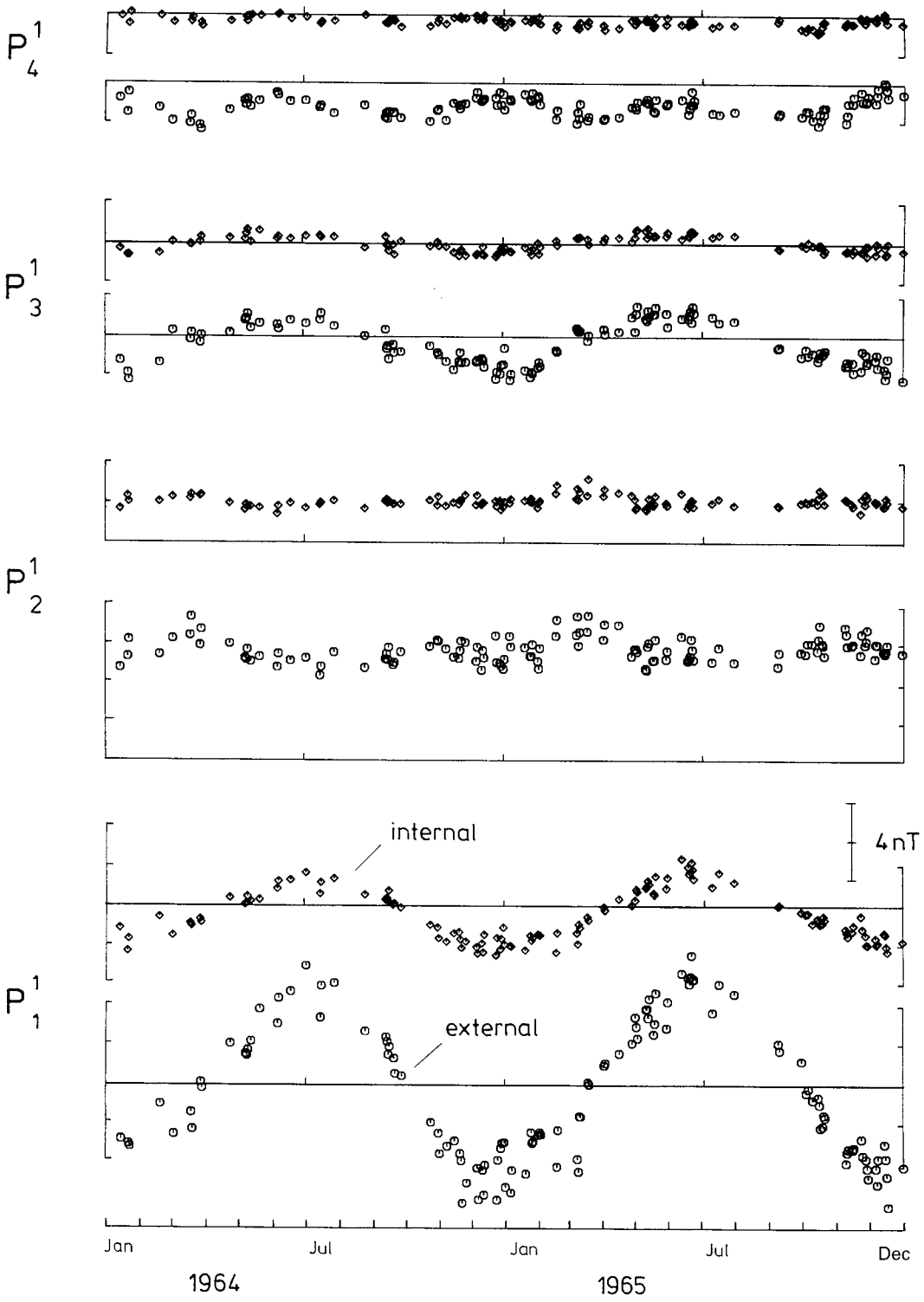

Figure 3. Day-to-day and seasonal variability of potential coefficients of daily variations during the IQSY 1964–1965. Shown are the real parts of external (ϵ_n^m) and internal (ι_n^m) coefficients of four local-time terms, for the first time harmonic on 123 Q*-days. Coefficients for the first P_1^1 and third P_3^1 term display seasonal changes in the form of annual variations. Those of the second *principal* term P_2^1 are roughly constant, except for a small semi-annual modulation, which also appears in the fourth term P_4^1. Noteworthy is the good correspondence between seasonal and day-to-day changes of external and internal potential coefficients in all four displays.

for the absolute term of the potential, with a corresponding series for Z_0. Obviously, the coefficients u_n^0 (and z_n^0) are real valued. Hence with the same choices $K = 4$ and $L = 1$ as series parameters, three real and four complex coefficients have to be derived for a least-squares fit to globally observed absolute values X_0, Y_0 and Z_0.

In this context no further detailed studies of *Sq* sources and their seasonal changes are intended. Instead, four representative

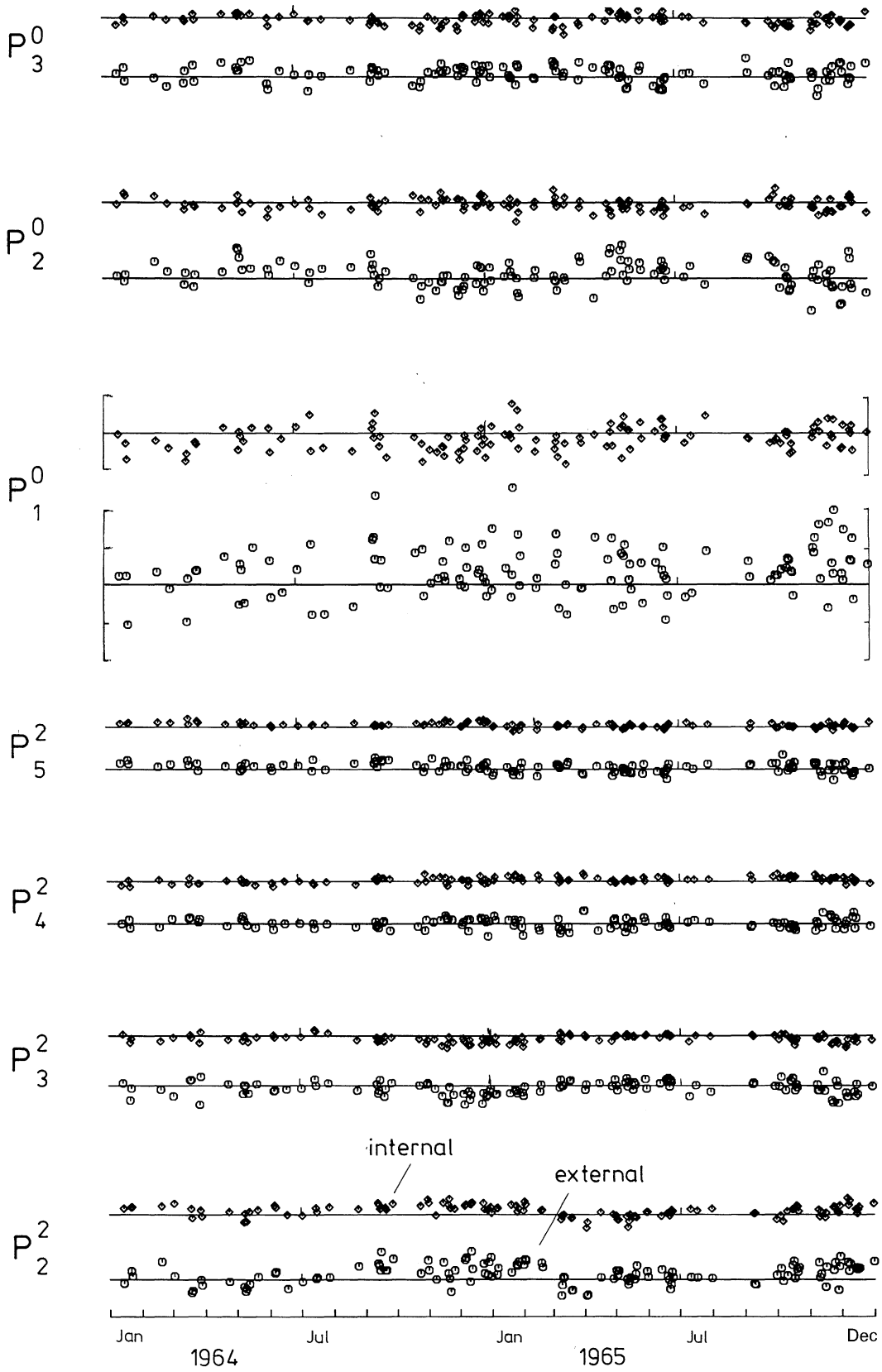

Figure 4. Day-to-day and seasonal variability of potential coefficients of daily variations during the IQSY 1964–1965, as in Fig. 3, but for the eight general terms, which take account of dependencies on longitude. The seasonal changes are less systematic than for local-time term coefficients, but the good correlation between changing external and internal coefficients is preserved. Scattered results for the Universal-time term P_1^0 may reflect transient contributions from *Dst*.

days are chosen during prolonged times of extreme magnetic quietness, one for each season. They resemble quiet-time solar daily variations *Sq* as closely as possible during equinoxes and solstices, here in years of minimum solar activity. Disturbed periods are at least four days away and any still-existing *Dst* contribution should have been eliminated by the non-cyclic change corrections (see Section 3 of Part I). Furthermore, lunar corrections have been applied in an attempt to represent truly solar daily variations on the chosen days (see Appendix B). The chosen dates and the respective eight three-hourly *Kp* indices for activity can be found in Table 9.

In the thus established absence of activity, contaminations by S_D or substorms should be negligible. Table 10 lists the external coefficients for these days, including those for the absolute terms. It may be added that with the choice of single days, rather than monthly or seasonal means, an attempt has been made to avoid any complications by taking an average over a possibly changing spatial structure from day to day. Figs 3 and 4 demonstrate that even within a single month substantial changes can occur, notably in the P_1^1 local-time term.

For visualization of the table entries, contours of a current function Ψ will be displayed in a sequence of global maps. This function depicts in $\mathbf{j} = -\hat{\mathbf{r}} \times \text{grad}\,\Psi$ the sheet current density of fictitious currents which flow in a thin shell just above the Earth's surface and could account for the external part of the surface field. With $\hat{\mathbf{r}}$ as unit vector in the radial direction, these 'equivalent' currents flow parallel to contours $\Psi = \text{const}$—clockwise around minima and anticlockwise around maxima of Ψ.

Assuming that U and Ψ are expressed by series of spherical harmonics of matching degrees and orders, the conversion of the external potential coefficients into those of the current function can be carried out term by term according to

$$w_n^m = -(R/\mu_0)\frac{2n+1}{n+1}\epsilon_n^m, \tag{14}$$

where w_n^m denotes the expansion coefficients for Ψ (see Chapman & Bartels 1940; Section 17.18). With $\mu_0 = 4\pi \times 10^{-7}$ V s A^{-1} m^{-1} and $R = 6371$ km as the Earth's radius, $R/\mu_0 = 5070$ A nT^{-1}. The insertion of ϵ_n^m from eq. (2) yields w_n^m directly in terms of the series coefficients for U and Z:

$$w_n^m = -(R/\mu_0)[u_n^m + z_n^m/(n+1)] \tag{15}$$

or, alternatively, with an earth model response

$$w_n^m = -(R/\mu_0)[1 + nC_n/R]u_n^m. \tag{16}$$

The last relation is readily inferred from eq. (4), replacing c_n^m by C_n for a laterally uniform earth. It suggests relatively small contributions from the Z expansion coefficients, noting that for the principal terms $n|C_n|$ is between one-fifth and one-third of R, as seen from Table 8.

The complementary conversion formulas, when the internal part of the surface field is to be represented by fictitious currents in a thin shell just below the Earth's surface, are

$$w_n^m = +(R/\mu_0)\frac{2n+1}{n}\iota_n^m = (R/\mu_0)[u_n^m - z_n^m/n] \tag{17}$$

or, alternatively,

$$w_n^m = (R/\mu_0)[1 - (n+1)C_n/R]u_n^m. \tag{18}$$

Hence, except for a change in sign, nearly the same current function can be expected as for the external part, since the penetration depth will be small enough to give $(n+1)C_n| \ll R$ for all terms.

The global display of the current function refers in the usual manner to the external field at a certain instant in Universal time t. Hence, a combined spherical and time harmonic synthesis is required to derive Ψ at this time for a specified global mesh of surface locations. With t in angular measure,

$$\Psi(t, \theta, \lambda) = \Psi_0(\theta, \lambda) + \sum_{p=1}^{6} \mathscr{R}e\{\Psi_p(\theta, \lambda)\, e^{ipt}\}, \tag{19}$$

where

$$\Psi_0(\theta, \lambda) = \sum_n w_n^0(0) P_n(\cos\theta) + \sum_{m,n} \mathscr{R}e\{w_n^m(0)\, e^{im\lambda}\} P_n^m(\cos\theta),$$
$$\Psi_p(\theta, \lambda) = \sum_{m,n} w_n^m(p)\, e^{im\lambda} P_n^m(\cos\theta). \tag{20}$$

The summations are those of eq. (13) of this article and eq. (6) of Part I. The resulting contours in Fig. 5 are for the time instant $t = \pi$, corresponding to noon in Universal time, and are shown on a global map which extends from local midnight to local midnight at that hour, with local noon on the Greenwich meridian in the centre. In carrying out the time harmonic synthesis it has been observed that, for the calculated Fourier coefficients, zero time is one-half hour past midnight.

The contour lines on the four chosen days resemble very faithfully the well-known pattern of *Sq* source currents in the four seasons. As in Parkinson's (1977) analysis, an attempt has been made to refer them to a genuine true zero level of no overhead currents, provided the underlying assumption is correct that any deviations from this level at local midnight are caused solely by internal currents. This differs from the common practice to add, quite arbitrarily, a longitude-independent value to the current function in all latitudes to obtain a constant Ψ along the midnight meridians of the display.

Except for the chosen December day, the night hours are indeed relatively free from overhead currents, which on the daylight side form two current loops north and south of the equator, with centres one hour before noon. The cause of the late evening currents on the December day is not clear. They may be an artefact, arising from deficiences in the separation of absolute terms and thus faulty zero levels. Total currents, inferred from the difference between maximum and minimum values of the current function, are more or less of the same strength in all four seasons, but a certain enhancement during equinoxes is indicated. Even though no data from the

Table 9. Dates and 3-hourly magnetic activity indices Kp of the four quiet days, for which external potential coefficients are listed in Table 10.

1964	September	20	Kp =	0o	0o	0o	0+	0+	0+	1-	1+
1964	December	23		1-	2o	2o	1-	1o	1-	0+	1+
1965	March	19		2o	0o	0-	2o	2+	1-	2-	1+
1965	June	21		0+	0+	0o	0+	0+	0+	0o	0+

Table 10. External potential coefficients $\epsilon_n^m(p)$ of lunar-corrected daily variations on four single quiet days during equinoxes and solstices (*cf*. Table 9). 12 (11) complex coefficients are listed for each of the four time harmonics $p=1$ to $p=4$, three real and four complex coefficients for the absolute term $p=0$. Series expansion according to eqs (6) and (8) of Part I, with ϵ_n^m for u_n^m. Coefficients are in nT and refer to quasi-normalized spherical functions according to A. Schmidt.

			1964 Sep 20	1964 Dec 23	1965 Mch 19	1965 Jun 21
p = 1	n	m				
	1	1	349 + 1001i	−5541 − 1994i	−174 + 878i	5193 + 1915i
	2	1	4488 + 1810i	5858 + 3135i	6947 + 2218i	4893 + 1828i
	3	1	−649 − 706i	−2125 − 413i	120 − 140i	1476 − 131i
	4	1	−1406 − 276i	−973 + 269i	−1780 + 286i	−1019 − 285i
	2	2	199 + 1181i	242 + 2077i	−761 + 927i	−524 − 334i
	3	2	−359 + 870i	−1121 + 177i	172 + 786i	482 − 286i
	4	2	358 − 951i	627 − 1008i	−229 − 1131i	205 − 551i
	5	2	422 + 380i	−43 + 452i	329 + 219i	−164 + 295i
	1	0	1689 − 509i	182 + 783i	−940 − 1999i	497 + 275i
	2	0	−518 + 1663i	−884 + 1983i	−734 + 2735i	249 + 389i
	3	0	113 + 19i	682 − 170i	344 − 367i	−281 − 1192i
p = 2	n	m				
	2	2	725 − 999i	100 + 743i	−40 − 270i	−622 − 1998i
	3	2	−1877 − 1860i	−2796 − 2362i	−3235 − 1699i	−2549 − 1662i
	4	2	241 + 637i	813 + 489i	−325 − 154i	−1054 − 383i
	5	2	233 + 417i	475 + 302i	239 + 383i	−47 + 6i
	3	3	−561 − 504i	230 − 898i	364 − 2i	355 + 360i
	4	3	697 − 163i	732 − 45i	199 − 503i	−217 + 82i
	5	3	−632 + 427i	−338 + 414i	−167 + 573i	−140 + 371i
	6	3	30 − 275i	−33 − 227i	−14 − 508i	165 − 387i
	1	1	−599 − 606i	66 + 3423i	280 + 1600i	−539 + 443i
	2	1	−1000 + 82i	36 − 323i	−175 − 157i	0 + 24i
	3	1	−59 − 875i	−83 − 707i	542 − 787i	−192 − 186i
	4	1	−266 − 110i	−12 − 151i	175 − 68i	224 + 409i
p = 3	n	m				
	3	3	−979 + 578i	161 − 338i	121 + 133i	−533 + 925i
	4	3	631 + 1376i	1004 + 1716i	1299 + 1460i	806 + 680i
	5	3	−144 − 423i	−339 − 282i	7 + 201i	113 + 144i
	6	3	75 + 52i	−136 − 172i	24 + 34i	266 + 52i
	4	4	141 + 373i	−364 + 241i	−190 − 255i	−9 − 153i
	5	4	−250 + 51i	−211 + 2i	20 + 64i	146 − 76i
	6	4	442 − 99i	141 − 234i	159 − 183i	163 − 98i
	7	4	−190 + 142i	−29 + 173i	−82 + 164i	−174 + 159i
	2	2	−264 + 346i	−455 − 768i	−96 − 170i	91 + 124i
	3	2	413 + 50i	−282 − 171i	164 + 219i	221 − 17i
	4	2	−269 + 374i	17 + 175i	−456 + 150i	−44 + 271i
	5	2	237 + 122i	−36 + 141i	233 + 19i	−33 − 202i
p = 4	n	m				
	4	4	286 − 48i	−172 − 367i	−222 + 11i	456 − 141i
	5	4	−2 − 544i	−42 − 620i	−273 − 609i	−23 + 9i
	6	4	132 + 159i	46 − 58i	86 − 82i	177 + 8i
	7	4	−5 − 131i	−62 + 89i	−57 + 2i	−143 − 41i
	5	5	−18 − 148i	258 − 36i	−42 + 218i	−42 − 40i
	6	5	43 + 5i	115 + 43i	−19 − 41i	−85 + 39i
	7	5	−209 − 67i	−104 + 41i	−168 + 64i	−77 + 66i
	8	5	95 − 86i	−30 − 102i	98 − 92i	106 − 23i
	3	3	64 − 69i	−43 + 342i	−26 − 92i	−104 − 52i
	4	3	−117 + 13i	134 + 110i	136 − 92i	−177 − 71i
	5	3	196 − 100i	−115 − 15i	220 − 60i	28 − 157i
	6	3	−166 − 41i	37 − 60i	−75 − 92i	22 + 75i
p = 0	n	m				
	1	0	−2690	−3777	−3782	−3817
	2	0	657	178	17	839
	3	0	2768	1909	3992	2754
	1	1	−40 − 464i	−651 − 2525i	281 − 386i	−36 − 54i
	2	1	−508 − 1223i	464 + 127i	−218 − 1014i	−438 + 63i
	3	1	−231 + 1443i	−284 + 1337i	−294 + 2043i	−773 + 54i
	4	1	−474 − 12i	−226 − 376i	−424 − 303i	−326 − 704i

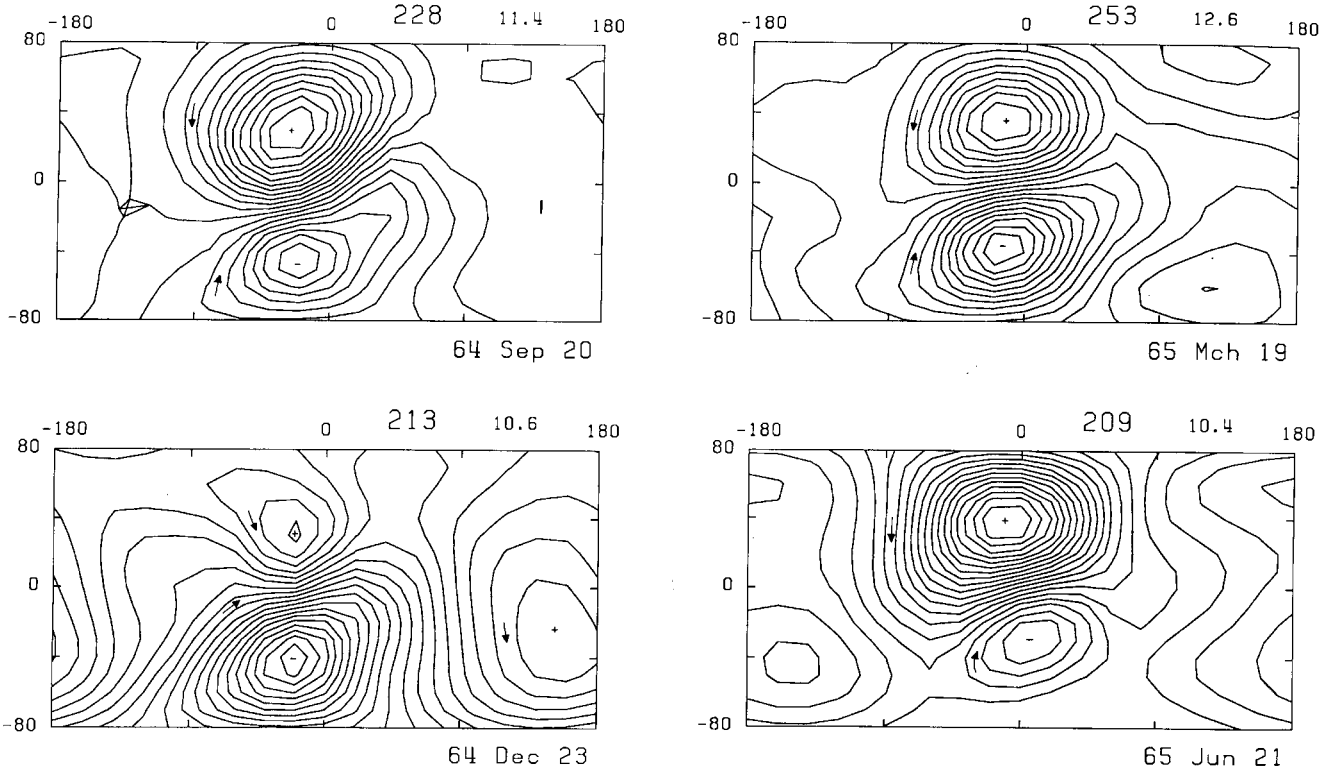

Figure 5. Equivalent currents for the external part of daily variations on four quiet days during equinoxes (upper diagrams) and solstices (lower diagrams). The global maps show contour lines of the current function at 12 hours Universal time and extend from midnight to midnight meridians. The time harmonic synthesis involves an absolute term and six Fourier coefficients, the preceding spherical harmonic synthesis 12 spherical harmonic terms for each Fourier coefficient. Large integer numbers on the upper right of each map give the total current between extrema, in kA, followed by smaller decimal numbers for the current between contour lines. The inclusion of separated absolute terms yields current loops, which are limited to the daytime hours in each hemisphere, with spurious and presumably unrealistic currents during the night. Current loop centres lie between 10.4 hours for the chosen day in mid-September and 11.1 hours for the chosen day in mid-March. Total currents are slightly stronger during equinoxes than during solstices. The influence of the course of the dip equator between Africa and South America on the external currents near noon is clearly seen. (*cf*. Fig. 1 in Part I.)

equatorial jet region were used, low-latitude currents near noon follow the course of the dip equator from Africa across the Atlantic (see Fig. 1 of Part I). Noting the well-established influence of the dip equator on the *Sq* system, this suggests that the derived longitude-dependent general terms have indeed a physical meaning.

Fig. 6 repeats the display of equivalent currents for the chosen day in March in order to illustrate various points. In the upper left map, the time instant of synthesis is shifted to zero hours and thus local noon is now at 180° longitude. The total current is about the same as 12 hr later, but the current pattern has changed to adapt most convincingly to the course of the dip equator in the Pacific (*cf*. Fig. 1 of Part I). The lower left map is the result of a spherical harmonic synthesis with four local-time terms only and thereby does not refer to any particular instant in Universal time. The total current remains unchanged, but low-latitude currents now flow parallel to the geographical equator and vividly reflect the missing influence of corrective longitude-dependent general terms.

In the remaining two maps, those terms are included again. The upper right map, for a synthesis without absolute terms, has the purpose of showing the strong influence that these terms have on the overall appearance of the contour lines. The prominent, but misleading current loops during night hours simply result from the choice of daily means as zero reference levels. The lower right map, finally, displays the associated pattern of equivalent internal currents, which closely resembles the external current flow, as expected. There is, however, a reduction of their total strength to about one-half. Current centres are displaced westwards by about 15°, which agrees with the postulated phase lead of induced currents from inducing currents.

No clear indications are visible for ocean effects or any other localized distortions of the current flow to internal induction anomalies. There is, however, evidence for the postulated flow of internal currents across the midnight meridians. Their presence verifies that the separation of absolute terms has indeed led to appropriate zero reference levels. It should be added that the synthesis of the internal current function does not include the internal part of the absolute terms. As time-constant internal contributions, they are assigned to the Earth's quasi-permanent field.

4 CONCLUDING REMARKS

The results are beyond expectations, which were low for progress in global induction research. The critical part of the potential method applied here remains the necessity of expressing the vertical component by a series of spherical harmonics. Whereas time harmonics of horizontal components

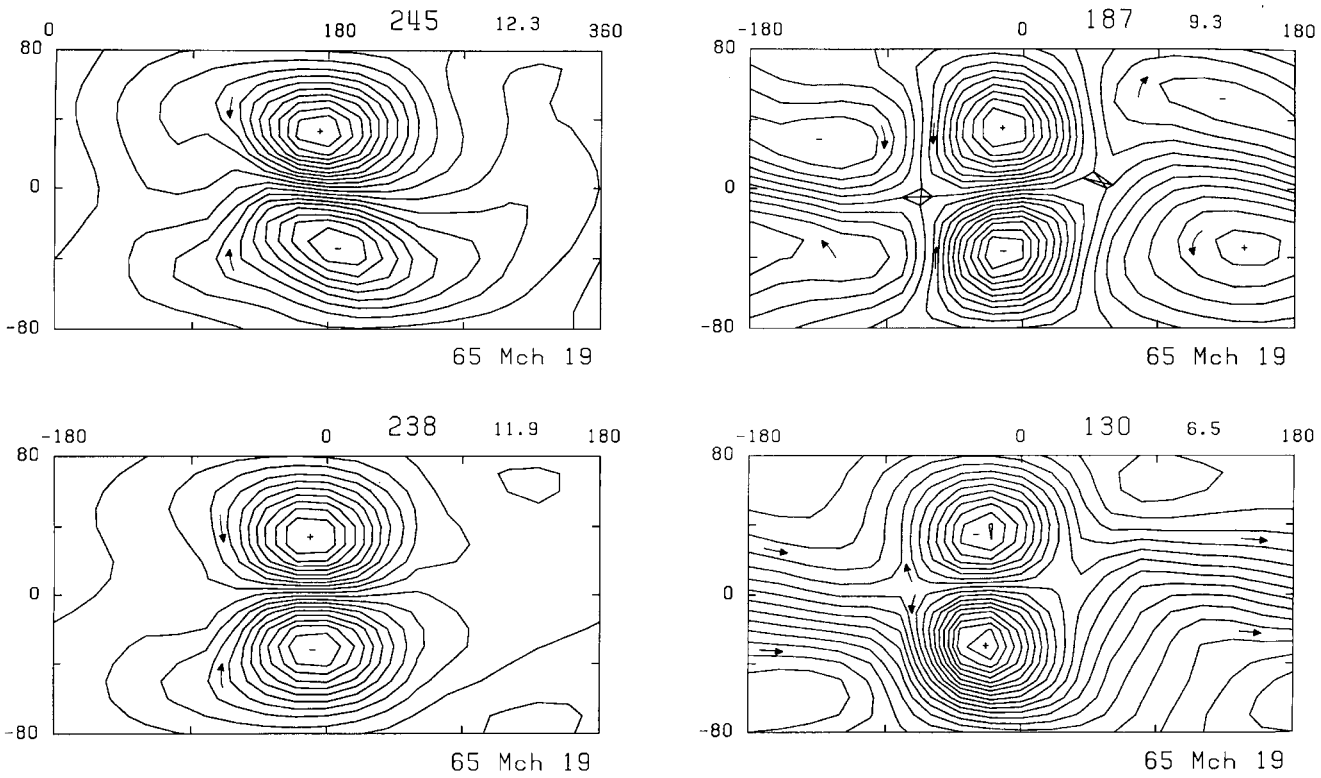

Figure 6. Equivalent currents as in Fig. 5 for daily variations on 19 March 1965. Upper left: external currents at zero hours Universal time UT, with local noon at 180°, to demonstrate the influence of the changed course of the dip equator in the Pacific region. Lower left: external currents at any hour UT, when only local-time terms are used in the spherical harmonic synthesis, demonstrating the physical significance of the omitted general terms in including longitude dependence. Upper right: external currents at 12 hours UT, when the synthesis is carried out with time harmonics only, omitting the absolute external term. Strong current loops during the night hours demonstrate the inappropriate choice of the daily means as zero reference level for daily variations. Lower right: internal currents at 12 hours UT. Their total strength is reduced by one-third in comparison to the external current on that day. Current centres in both hemispheres are shifted westwards to 10.2 hours local time, while external current centres are at 11.1 hours, demonstrating the phase shift between inducing external and induced internal sources (*cf*. Fig. 5). Substantial internal currents cross the midnight meridians (see text). There are no clear indications for ocean effects or other anomalies of internal origin.

appear as smoothly varying with latitude and longitude, those of the vertical component are scattered, as to be expected from their greater sensitivity to induction anomalies of internal origin. In the southern hemisphere they are without any visible indications of a large-scale global structure. Here almost all observatories are either on islands or coastlines and thus fully exposed to anomalous effects from the ocean. Clearly, no polynomial in latitude and longitude, with a realistic number of terms, could reproduce such observations without large residuals.

Still, it has been possible to establish statistically significant and physically meaningful relationships between *all* coefficients of the two series, for the potential and the vertical component, which in quite different proportions account for the observed horizontal and vertical fields, respectively. High coherencies testify to a surprising stability of these relations, even though the spatial structure of the inducing source changes from day to day and with the seasons. The very fact that such generally valid univariate term-by-term relations exist is a remarkable result in itself and by no means self-evident.

The implication for the internal conductivity structure can only be that neither ocean effects nor lateral non-uniformities within the depth range of penetration of daily variations are strong enough to invalidate interpretations with radially symmetric earth models, for local-time responses more so than for those not in local time. These results emphasize the special advantage that daily variations provide for global induction studies. The fact that the analysis is concentrated on their westward-propagating mode, moving with the speed of the Sun, tends to suppress anomalous induction effects, fixed to the earth, and to accentuate the response of an *average* earth of radial symmetry.

However, it is unclear how the derived results translate into internal conductivities on a global scale, and the demonstrated compatibility with a layered earth model cannot be more than a first step of interpretation. Furthermore, results of this study may be biased towards conditions below continents in the northern hemisphere. It has to be left to on-going 3-D model studies, as in the accompanying article by Kuvshinov *et al.* (1999), to determine how the presence of oceans influences the sets of spherical harmonics derived here and whether the underlying upper mantle is indeed without traceable signs of lateral non-uniformity in ocean-corrected response estimates.

It is noteworthy already at this stage that responses for the various terms of a given harmonic do not diverge with increasing frequency, as one would expect for a spherical conductor that deviates from radial symmetry mainly in its outermost layers, but that they converge, as if such non-uniformities do not exist. The prospects are marginal, it seems, of testing this conclusion with higher frequencies. Such an

extension beyond 6 cpd would also be a prerequisite for learning more about mantle conductivities in the most interesting depth range from, say, 100 km to 300 km depth, which includes Gutenberg's seismic low-velocity layer. Experience has shown that the typical time–space structure of daily variations ends with their fourth harmonic at 4 cpd. The adjoining frequencies will reflect more and more spatially complicated source fields from polar jet regions and thereby will be less adaptable to global representation by spherical harmonics.

Disappointingly, two attempts failed to separate normal and anomalous responses—first by splitting pairs of spherical harmonics into travelling and standing parts, and second by a bi-variate formulation of the linear relation connecting coefficients of the two series. In either case the available database may have been insufficient. Both proposed separation schemes also need a firmer theoretical basis. Also disappointing is the lack of any significant improvement in the response estimates by applying day-by-day corrections for lunar daily variations. A repetition of their spherical harmonic analysis with matching sets of spherical terms, as used in this study, may lead to better results.

The separation of external and internal parts involves no *a priori* assumptions and therefore is without comparable fundamental uncertainties. It appears that representative external fields for the four seasons have been derived to be utilized as inducing sources for global model studies. Similar analyses are needed for years of maximum Sunspot numbers to supplement Parkinson's (1977) and Malin's (1973) work on the IGY data, the latter being restricted to solar daily variations in their annual means. A particular point of interest would be a comparison of seasonal changes of individual spherical harmonic coefficients, as found in this study for the IQSY.

Unfortunately, the permissible number of spherical harmonics is too small to resolve adequately the internal field, including distorting effects from oceans and possibly also mantle inhomogeneities. Here progress has to await an improved hemispherical balance and a more suitable positioning of sites of observation. The eigenvalue decomposition has shown how effectively the number of terms can be increased with a more even distribution of observatories, while the comparison of results from different data sets has demonstrated that simultaneous global observations of not too many quiet days would suffice.

Altogether, this return to the classical potential method has been a rewarding experience and an invitation to include into future analyses lunar daily variations and smoothed storm-time *Dst* variations. These results would supplement and test those from other methods in the pursuit of a better understanding of the global induction process, a prerequisite to deciphering the deep conductivity structure of the Earth.

ACKNOWLEDGMENTS

In the same way as this study would not have been possible without the dedicated work carried out at geomagnetic observatories in many countries, it would equally not have been possible without the admirable work by Dr Dennis E. Winch, University of Sydney, who collected the observatory hourly mean values for the IQSY and prepared them for use by others. Thanks are also due to Dr Edward B. Fainberg, Geoelectromagnetic Research Institute of the Russian Academy of Sciences, who kindly supplied additional data from his own collection for 1965. I am indebted to Dr Alexei V. Kuvshinov, who initiated my return to the subject and was very instrumental in the ultimate completion of this work. Dr Nils Olsen and four reviewers have made the most valuable comments and pointed out numerous errors and obscure expressions. I am grateful in particular to Dr Roger Banks for his help to improve the original version of Part II.

REFERENCES

Berdichevsky, M.N., Fainberg, E.B., Rotanova, N.M., Smirnov, J.B. & Vanjan, L.L., 1976. Deep electromagnetic investigations, *Ann. Geophys.,* **32,** 143–155.

Campbell, W.H. & Anderssen, R.S., 1983. Conductivity of the subcontinental Upper Mantle: an analysis using quiet-day geomagnetic records of North America, *J. Geomag. Geoelectr.,* **35,** 367–382.

Campbell, W.H. & Schiffmacher, E.R., 1988. Upper Mantle electrical conductivity for seven subcontinental regions of the Earth, *J. Geomag. Geoelectr.,* **40,** 1387–1406.

Chapman, S., 1919. The solar and lunar diurnal variation of the earth's magnetism, *Phil. Trans. R. Soc. Lond.,* A, **218,** 1–188.

Chapman, S. & Bartels, J., 1940. Geomagnetism, Clarendon Press, Oxford.

Fainberg, E.B. & Berdichevsky, M.N., 1977. Deep magnetovariation profiling with the method of derivatives, *Acta Geodaet., Geophys. et Montanist. Acad. Sci. Hung.,* **12 (1–3),** 377–391.

Jenkins, G.M. & Watts, D.G., 1968. *Spectral Analysis and its Application,* Holden-Day, San Francisco.

Kuvshinov, A.V., Avdeev, D.B. & Pankratov, O.N., 1999. Global induction by Sq and Dst sources in the presence of oceans: bimodal solution for non-uniform spherical surface shells above radially symmetric Earth models in comparison to observations, *Geophys. J. Int.,* submitted.

Lahiri, B.N. & Price, A.T., 1939. Electromagnetic induction in non-uniform conductors, and the determination of the conductivity of the earth from terrestrial magnetic variations, *Phil. Trans. R. Soc. Lond.,* A, **784,** 509–540.

Larsen, J.C., 1989. Transfer functions: smooth robust estimates by least-squares and remote reference methods, *Geophys. J. Int.,* **99,** 645–663.

Malin, S.R.C., 1973. Worldwide distribution of geomagnetic tides, *Phil. Trans. R. Soc. Lond.,* **274,** 551–594.

Olsen, N., 1998. The electrical conductivity of the mantle beneath Europe derived from C-responses from 3 h to 720 h, *Geophys. J. Int.,* **133,** 298–308.

Parkinson, W.D., 1977. An analysis of the geomagnetic diurnal variations during the International Geophysical Year, *Bulletin 173,* Australian Government Publ. Service, Canberra.

Schmucker, U., 1970. Anomalies of geomagnetic variations in the Southwestern United States, *Bull. Scripps Inst. of Oceanography,* vol. 13, University of California.

Schmucker, U., 1984. Elektromagnetische Übertragungsfunktionen für tagesperiodische Variationen, in *Protokoll Koll. Elektromagnetische Tiefenforschung Grafrath,* pp. 11–33, eds. Haak, V. & Homilius, J., Nieders. Landesamt f. Bodenforschung, Hannover.

Schmucker, U., 1985. Magnetic and electric fields due to electromagnetic induction by external sources, in *Landolt-Börnstein Numerical data and functional relationships in Science and Technology. New Series Group V, 2b,* pp. 100–125, eds Fuchs, K. & Soffel, H., Springer Verlag, Berlin.

Schmucker, U., 1999. A spherical harmonic analysis of solar daily variations in the years 1964–1965: response estimates and source fields for global induction—I. Methods, *Geophys. J. Int.,* **136,** 439–454 (this issue).

Winch, D.E., 1981. Spherical harmonic analysis of geomagnetic tides, 1964–65, *Phil. Trans. R. Soc. Lond.,* **303,** 1–104.

APPENDIX A: THE SINGLE-DAY UNIVARIATE LINEAR REGRESSION ANALYSIS

In the linear expression

$$y_n(\omega_p) = c(\omega_p)x_n(\omega_p) + \delta y_n(\omega_p) \tag{A1}$$

the variables y_n and x_n are either complex time harmonic or complex spherical harmonic coefficients. The subscript n refers to the nth day, in an assemblage of N single days; the subscript p, to the pth time harmonic of daily variations with $\omega_p = 2\pi p \text{ day}^{-1}$. The least-squares estimator for the transfer function $c(\omega_p)$ and its error are

$$\begin{aligned} c &= [yx^*]/[xx^*], \\ \Delta c^2 &= |c|^2\epsilon^2[(1/\beta)^{1/m} - 1]/\text{coh}^2, \end{aligned} \tag{A2}$$

with $m = N - 1$, and with

$$\begin{aligned} \text{coh}^2 &= [yx^*]^2/[xx^*][yy^*], \\ \epsilon^2 &= 1 - \text{coh}^2 = [\delta y \delta y^*]/[yy^*] \end{aligned} \tag{A3}$$

as the squared coherency and the squared residual of the linear regression, respectively. Square brackets $[\ldots]$ imply summation of Fourier products over the N days, and $(1-\beta)$ is the probability that modulus $|c|$ lies within error limits $|c| \pm \Delta c$. Because unsmoothed Fourier products of harmonic coefficients are added, the degrees of freedom of the relevant F-distribution to estimate errors are $\nu_1 = 2$ and $\nu_2 = 2m$, which allows the required integration of the pertinent probability density function $f(q) = [m/(m+q)]^{m+1}$ to be carried out in closed form. The general formula to derive confidence intervals for the modulus of univariate transfer functions can be found as eq. (10.3.18) in Jenkins & Watts (1968).

The error estimate presumes that the residuals, transformed back into time series, are independent, normally distributed random variables of zero mean and of the same variance σ^2 at each of the P instants of time involved, here at $P = 24$ hours. In order to strengthen the validity of the resulting *statistical* error limits, all Fourier products are multiplied with weights $q_n(\omega_p)$ for a given day and time harmonic. The estimation of $c(\omega_p)$ begins with weights $q_n = 1$ for all days and harmonics. From the resulting estimator $c^{(0)}$ and residuals $\delta y_n^{(0)} = y_n - c_n^{(0)} x_n$ a first set of weights is calculated, as described below.

The analysis is carried out again with weighted Fourier products and repeated until an unchanging set of weights evolves, which in this study never required more than four iterations. It has been decided to preserve weights once they have been derived; that is, if a certain day and harmonic already has a weight from one or more previous cycles, then the weight for the next cycle will be the product of the old and newly derived weights.

If the (weighted) residuals δy_n are the time harmonics of random variables at P instances of time, then their real and imaginary parts should be normally distributed with zero mean and variances σ^2/M, where $M = P/2$ and $P = 24$. Thus, the normalized sum of their squares,

$$u_n = M|\delta y_n|^2/\sigma^2 \quad \text{with} \quad |\delta y_n|^2 = q_n|y_n - cx_n|^2, \tag{A4}$$

should be χ^2-distributed with two degrees of freedom. Its probability density function $\exp\{-u_n/2\}/2$, integrated from $u_n = u_{nL}$ to infinity, gives in $u_{nL} = 2\log(1/\beta)$ an easily derivable limit, which u_n exceeds with probability β.

The days are now grouped into nine classes $I = 0, 1, 2, \ldots, 8$ according to the size of their weighted squared residuals, and class assignments are chosen to be

$$I = \min\{8, \text{int}[u_n/\log 10]\}. \tag{A5}$$

Hence, the chance that a day is in the open-ended last class of the worst fit is with $\beta_8 = 1:10000$ for $u_n \geq 8 \log 10$ exceedingly small, and, in the case of, say, 100 days very unlikely. Class $I = 0$ of the best fit should contain about two-thirds of the days, with probability $\beta_0 = 1 - 1/\sqrt{10} = 0.684$ that u_n is below $\log 10$. Probabilities for the remaining classes are

$$\beta_I = 10^{-I/2} - 10^{-(I+1)/2}. \tag{A6}$$

All N_I days in class I receive the weights $q_n = \beta_I N^*/N_I$, where N^* is the sum of weights from the previous cycle (N in the initial cycle), and $\beta_I N^*$ is the expected number of days in class I. It has been found that, whenever a day is not within the first four classes, it is usually assigned to the two highest classes, which identifies this day as a clear outlier.

Following the rules of robust statistics, no weights greater than unity are given and up to a certain threshold probability all days receive unit weights. After tests it has been decided to use unit weights for days in the first three classes, with a joint probability $\beta_0 + \beta_1 + \beta_2 = 1 - 1/\sqrt{1000} = 0.968$ slightly above the 2σ limit of a normal distribution.

Other methods of weighting have been tried, but the method described here, based on observed and expected occupancies of classes, appears to be preferable. It follows Larsen's approach of implementing data-adaptive weights (Larsen 1989; Section 3.3). In some cases more than one-half of the days had to be eliminated, even though this was experienced only in applications of the $Z:Y$ method.

The required estimation of the variance σ^2 in eq. (A4) is has follows. By extending the time harmonic analysis to the Nyquist frequency ω_M, Parseval's theorem yields in the sum of squared residuals over *all harmonics* on a given day an estimate s_n^2 for σ^2 on that day, after division by two. In $\epsilon^2[qyy^*]$, the sum of weighted squared residuals over *all days* is known from the least-squares solution, as seen from eq. (A3). Hence, after changing the sequence of summations,

$$s^2 = \frac{1}{2}\sum_{p=1}^{M}\left\{\epsilon^2(\omega_p)\left[\sum_{n=1}^{N} q_n(\omega_p)|y_n(\omega_p)|^2\right] \Big/ N^*(\omega_p)\right\} \tag{A7}$$

represents a weighted mean of variance estimates s_n^2 on the N days. It has been used as an estimator of σ^2, when the residuals δy_n are time harmonics, as in the $Z:Y$ method.

For the reasons stated earlier, a Fourier synthesis towards time-domain residuals is problematic in the case of the potential method. As a substitute, daily estimates $s_n^2 = M|\delta y_n|^2/2$ are used by assuming that all time harmonics have the same residual on a given day. Their weighted mean

$$s^2(\omega_p) = \frac{M}{2}\epsilon^2(\omega_p)\left[\sum_n \ldots\right] \Big/ N^*(\omega_p) \tag{A8}$$

provides then a frequency-dependent estimator for σ^2.

APPENDIX B: LUNAR CORRECTIONS OF DAILY VARIATIONS

Two timescales are involved, both hereafter in angular measure: local lunar time τ and local solar time $T = \tau + \nu$, with ν

denoting the phase of the Moon. For simplicity, this will be the lunar phase at local noon on the considered day. Semi-diurnal lunar tides have time factors $\exp\{2i\tau\} = \exp\{2i[T-v]\}$, while ionospheric conductivity σ_I, a prerequisite for motion-induced currents, depends on local solar time. It will be expressed by a Fourier series

$$\sigma_I(T) = \sum_{n=-N}^{N} a_n \, e^{inT}, \tag{B1}$$

with $a_{-n} = a_n^*$ for a real-valued conductivity.

It has been found that lunar daily variations are best described by harmonics with time factors $\exp\{i[(2+n)T-2v]\}$, which is the product of the stated time factors for semi-diurnal tides and ionospheric conductivity. For $n = -1, 0, +1, \ldots, N$ they are known as Chapman's 'phase-law' tides. If the choice is $N \geq 3$, then additional 'partial' tides, in Schneider's terminology, are present with $n = -N, -N+1, \ldots, -3$. The long periodic constituent with $\exp\{-2iv\}$ for $n = -2$ and the choice $N \geq 2$ has no connection to daily variations.

Both tides contribute to daily variations in local solar time: phase-law tides with time factors $\exp\{i[pT-2v]\}$, setting $p = 2+n$, and partial tides with $\exp\{-i[pT+2v]\}$, setting $p = -(2+n)$. It will be assumed that from global observations extracted lunar daily variations have been developed into series of spherical harmonics and that for the pth time harmonic sets of lunar coefficients $u_n^m(L, p)$ and $z_n^m(L, p)$ in reference to $v = 0$ are available. Multiplied by the appropriate phase factor, which is $\exp\{-2iv\}$ in the case of phase-law tides, they are the desired corrections for the coefficients $u_n^m(p)$ and $z_n^m(p)$ at lunar phase v. In this study, Winch's coefficients for the IQSY are used (Winch 1981; Table 8.4), including all available coefficients for phase-law tides and one leading coefficient for partial tides, the latter for $p = 1$, with $n = 1$ and $m = 0$. The relative size of the applied lunar connections can be inferred from Table 11.

APPENDIX C: ON THE SEPARATION OF TRAVELLING AND STANDING PARTS OF DAILY VARIATIONS

The following sum of westward- and eastward-travelling terms in a spherical harmonic expansion will be considered, omitting their common dependence on latitude:

$$S = A \, e^{i(pt + m\lambda + \alpha)} + B \, e^{i(pt - m\lambda + \beta)} \tag{C1}$$

with $m = 1, 2, \ldots$. The time factor $\exp(ipt)$ associates the sum with spherical harmonics for the pth time harmonic; A and B are positive real amplitudes and λ is longitude. With the notation

$$\sigma = (\alpha+\beta)/2, \qquad \delta = (\alpha-\beta)/2, \qquad \gamma = \delta + m\lambda \tag{C2}$$

the sum is transformed into

$$S = [A \, e^{i\gamma} + B \, e^{-i\gamma}] \, e^{i(pt+\sigma)} \tag{C3}$$

in preparation for the intended separation. If $A > B$, S is then readily decomposed into a westward travelling part with amplitude $A - B$ and a standing part with amplitude $2B$, and vice versa for $B > A$. Explicitly, the sum becomes

$$S = (A-B) \, e^{i(pt + m\lambda + \alpha)} + 2B(\cos\gamma) \, e^{i(pt+\sigma)} \tag{C4}$$

for $A > B$ and

$$S = (B-A) \, e^{i(pt - m\lambda + \beta)} + 2A(\cos\gamma) \, e^{i(pt+\sigma)} \tag{C5}$$

for $B > A$.

APPENDIX D: ON THE $Z:Y$ METHOD

Provided that the Earth is radially symmetric with respect to conductivity, then for a frequency ω_p the same response $c_n^m(\omega_p) = C_n(\omega_p)$ applies to all spherical harmonic source terms of degree n. Assuming this to be a valid supposition, a spherical

Table 11. Unseparated potential coefficients $u_n^m(p)$ of daily variations (S and L) on 16 October 1965, in comparison to coefficients $u_n^m(L, p)$ of lunar daily variations during the IQSY, for the second time harmonic $p = 2$ and 12 spherical harmonic terms. The lunar phase on the chosen day is $v = 343°$. Lunar coefficients for $v = 0$ are from Winch's (1981, Table 8.4) analysis. All entries in pT.

		m = p = 2		
	n = 2	3	4	5
$u_n^m(2)$	416 - 135 i	-4835 - 2458 i	355 + 67 i	385 + 510 i
$u_n^m(L,2)$	121 + 1 i	218 - 389 i	4 - 15 i	- 43 + 47 i
		m = p + 1 = 3		
	n = 3	4	5	6
$u_n^m(2)$	-815 - 982 i	391 + 46 i	-378 + 286 i	85 - 282 i
$u_n^m(L,2)$	109 + 121 i	23 + 35 i	-	-
		m = p - 1 = 1		
	n = 1	2	3	4
$u_n^m(2)$	-489 + 623 i	-41 + 254 i	549 - 1389 i	13 + 343 i
$u_n^m(L,2)$	-545 - 160 i	16 + 78 i	84 + 30 i	- 64 - 23 i

harmonic synthesis on either side of eq. (3), first over degrees and then over orders, yields

$$Z_p^*(\theta, \lambda) = \sum_n (n+1)n \frac{C_n(\omega_p)}{R} Y_n(p, \theta, \lambda), \tag{D1}$$

where

$$Y_n(p, \theta, \lambda) = \sum_m u_n^m(p) P_n^m(\cos\theta)\, e^{im\lambda}. \tag{D2}$$

The asterisk (*) identifies Z_p as the result of a spherical harmonic synthesis. Time factors are $\exp(ipt)$ in reference to Universal time t, and R is the Earth's radius.

With the further assumption that within the range of degrees involved the responses $C_n(\omega_p)$ more or less agree, because $n|C_n|$ is small compared with R in that range, they can be replaced by a degree-independent response $C_0(\omega_p)$. It may approximate either C_n for the leading term or simply the zero-wavenumber response of a plane earth. This assumption reduces eq. (D1) to

$$Z_p^*(\theta, \lambda) = \frac{C_0(\omega_p)}{R} \sum_n n(n+1) Y_n(p, \theta, \lambda). \tag{D3}$$

The identity

$$\sum_n n(n+1) Y_n = \left\{ \frac{\partial(\sin\theta B_\theta)}{\partial\theta} + \frac{\partial B_\lambda}{\partial\lambda} \right\} \Big/ \sin\theta \tag{D4}$$

connects eq. (D3) to the horizontal gradient method to derive local response estimates. Eq. (D4) is readily verified by a term-by-term differentiation of the series eq. (10) of Part I for $B_\theta(= -X_p)$ and $B_\lambda(= Y_p)$, using eq. (8) of Part I and observing that for associated spherical harmonics

$$\frac{d(\sin\theta dP_n^m/d\theta)}{\sin\theta d\theta} + \left[n(n+1) - \frac{m^2}{\sin^2\theta} \right] P_n^m = 0. \tag{D5}$$

Berdichevsky *et al.* (1976) used eq. (D3) to derive, from a given set of spherical harmonic coefficients for U and Z, the depth

$$h_p(\theta, \lambda) = R\, \mathscr{R}e \left\{ Z_p^*(\theta, \lambda) \Big/ \sum_n n(n+1) Y_n(p, \theta, \lambda) \right\} \tag{D6}$$

of a perfect substitute conductor, which is the real part of C_0.

As indicated, this depth may vary for a given frequency from surface point to surface point. Hence, the results of a spherical harmonic analysis and subsequent synthesis can be represented by contours $h_p = \text{const.}$ on global maps, one for each frequency, to visualise the degree of spatial uniformity of the depth of penetration at the chosen frequency. Fainberg & Berdichevsky (1977) have in this way converted Malin's (1973) mean annual results for solar and lunar daily variations during the IGY into depth contours. Table 12 contains a similar map, but for the results of a single quiet day.

Table 12. Depth values of a perfect substitute conductor, in kilometres, for the first time harmonic of daily variations on 16 October 1965, derived from synthesized vertical components and horizontal gradients according to eq. (D6), with 12 spherical harmonic terms. Syntheses for 32 mid-attitude positions in both hemispheres.

	180W		90		0		90		180E
45.0N	590	599	711	790	743	665	601	574	590
22.5	539	557	607	656	692	702	664	587	539
22.5	373	552	390	462	469	447	406	403	373
45.0S	667	732	813	891	937	888	678	613	667

Outside the omitted polar and equatorial regions, where Z is too small for reliable determinations, more or less consistent depths are derived. Their mean value of close to 600 km agrees well with least-squares estimates. However no significance should be given to the displayed spatial variability of h_p because it follows from the ratio of two synthesized field quantities without the possibility of stating errors.

To permit a statistical evaluation, the spherical harmonic synthesis of the vertical component is avoided, replacing Z_p^* by Z_p from observations at a single site. This allows the reformulation of eq. (D1) as a univariate linear expression

$$Z_p(\theta, \lambda) = \frac{C_0(\omega_p)}{R} \sum_n n(n+1) Y_n(p, \theta, \lambda) + \delta Z_p(\theta, \lambda), \tag{D7}$$

between a locally observed Z_p and in effect the horizontal gradients of X_p and Y_p, synthesized from the spherical harmonics of the global potential. It is solved by least squares towards a best-fitting C_0 response estimate for an assemblage of events (days). The resulting estimate may be regarded as a 1-D approximation to the local inductive response at the point where Z has been observed. A correction factor $\gamma_n = C_n/C_0$ can be included under the sum, calculated for an *a priori* layered earth model, to account for the usually weak dependence of C_n on degree n.